The University of South Bohemia in České Budějovice
Faculty of Science

Validation of mitochondrial localization and essentiality of prioritized proteins assigned to the tripartite attachment complex in the protozoan parasite *Trypanosoma brucei*

Bachelor thesis

Jacqueline Bittner

Supervisor: Ignacio Miguel Durante, Ph.D.
Co-Supervisor: Mgr. Vendula Rašková

České Budějovice 2022

Bittner J., 2022: Validation of mitochondrial localization and essentiality of prioritized proteins assigned to the tripartite attachment complex in the protozoan parasite *Trypanosoma brucei*. Bc. Thesis, in English – 51 p., Faculty of Science, University of South Bohemia, České Budějovice, Czech Republic.

Annotation

During this thesis the localization of the prioritized proteins Tb927.11.13600, Tb927.11.14570, Tb927.4.840 and Tb927.6.4540 and their connection to the tripartite attachment complex of the protozoan parasite *Trypanosoma brucei* was examined to verify previous annotations found on the TrypTag database. Additionally, the essentiality of the prioritized proteins was evaluated.

Declaration

I declare that I am the author of this qualification thesis and that in writing it I have used the sources and literature displayed in the list of used sources only.

Place, date:
Student's signature:

Acknowledgement

I am extremely grateful to my supervisor Ignacio Durante for his support, expertise, and patience during both the experimental work and the writing process. He showed me how day-to-day research is done and the importance of doing everything with care.

I would also like to thank Vendula Rašková, who always was there when I needed help. Without her and her answers to my questions a lot of these experiments would have been failures.

At last, I want to thank Ambar Kachale for his friendship during my time in the lab. Our conversations were very entertaining and valuable to me and, at times, gave me new perspectives.

Above all I want to thank my family, who embraced my interest in science from the start and always supported me.

Table of Contents

Abbreviations

3-HMG-CoA	3-hydroxy-3-methylglutaryl coenzyme-A
AAT	Animal African trypanosomiasis
APRT	Adenine phosphoribosyltransferase
APS	Ammonium persulfate
ATP	Adenosine triphosphate
bp	Base-pair
BSA	Bovine serum albumin
CYTO	cytoplasmic
DAPI	4',6-diamidino-2-phenylindole
DNA	Deoxyribonucleic acid
DTT	Dithiothreitol
ECL	Enhanced chemiluminescence
E. coli	*Escherichia coli*
EDTA	Ethylenediaminetetraacetic acid
EGTA	Ethylene glycol-bis(β-aminoethylether)-N,N,N',N'-tetraacetic acid
FBS	Fetal bovine serum
g	gravitational force
gDNA	Genomic deoxyribonucleic acid
HAT	Human African trypanosomiasis
HCl	Hydrochloric acid
HRP	Horseradish peroxidase
Hsp70	70 kilodalton heat shock protein
Hsp90	90 kilodalton heat shock protein

IFA	Immunofluorescence assay
kb	Kilobase
KCl	Potassium chloride
KH_2PO_4	Potassium dihydrogen phosphate
LB	Lysogeny broth
lhRNAi	Long-hairpin ribonucleic acid interference
LicD	Lipooligosaccharide cholinephosphotransferase
$MgSO_4$	Magnesium sulfate
MITO	mitochondrial
NaCl	Sodium chloride
Na_2HPO_4	Disodium hydrogen phosphate
ORF	Open reading frame
PBS	Phosphate buffered saline
PBS-T	Phosphate buffered saline with Tween 20
PCR	Polymerase chain reaction
PVDF	Polyvinylidene difluoride
rcf	Relative centrifugal force
RISC	Ribonucleic acid induced silencing complex
RNA	Ribonucleic acid
RNAi	Ribonucleic acid interference
rpm	Revolutions per minute
RT	Room temperature
SDS	Sodium dodecyl sulfate
SDS-PAGE	Sodium dodecyl sulfate-polyacrylamide gel electrophoresis
SmOx	Single Marker Oxford

TAC	Tripartite attachment complex
TAE	Tris-acetate-ethylenediaminetetraacetic acid
T. brucei	*Trypanosoma brucei*
TEMED	Tetramethylethylenediamine
Tet	Tetracycline
TRIS	Tris(hydroxymethyl)aminomethane
Triton-X-100	2-[4-(2,4,4-trimethylpentan-2-yl)phenoxy]ethanol
UTR	Untranslated region
UV	Ultraviolet
vPBS	Voorheis' modified phosphate buffer saline
WB	Western blot
WCL	Whole cell lysate
x	times
YFP	Yellow fluorescent protein

1 Introduction

1.1 *Trypanosoma brucei* – sanitary relevance and life cycle

The parasite *Trypanosoma brucei* is a flagellated unicellular eukaryotic protist that belongs to the Kinetoplastida group and has three distinct varieties: *T. brucei brucei*, *T. brucei gambiense* and *T. brucei rhodesiense* [1,2]. Present in 36 African countries it infects both humans and animals, causing HAT, commonly known as African sleeping sickness, and AAT, also called Nagana, respectively [3]. Common symptoms include fever, an itching skin, inflammation of the lymph nodes and disturbances of the circadian rhythm, leading to the characteristic change of sleep patterns of patients. While *T. brucei brucei* is non-infectious towards humans due to a host immune response, infection with *T. brucei gambiense*, which accounts for more than 9 out of 10 of all HAT cases, and *T. brucei rhodesiense* are fatal without treatment. To date, no effective vaccines exist, and the drugs used for the medication of the disease report toxicities and may have no effects after application [4].

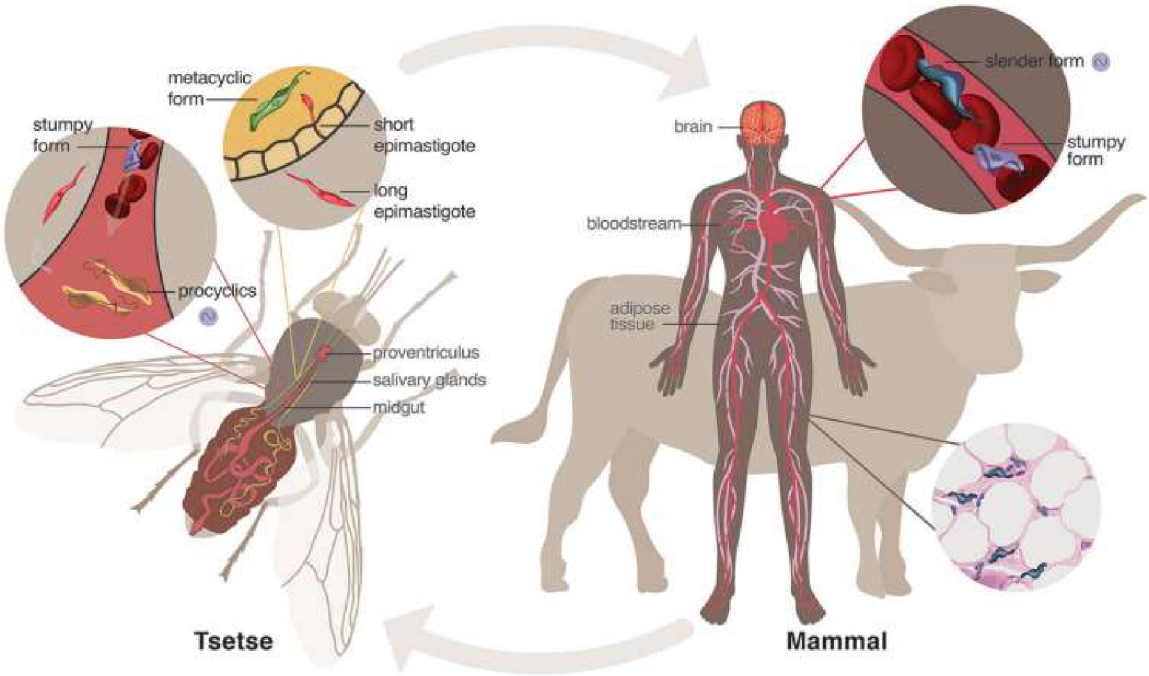

Figure 1: Depiction of *T. brucei* life cycle [4]

T. brucei is transmitted through tsetse fly bites and requires both the insect and a mammalian host for a full completion of its life cycle [4]. The mammalian host is infected with metacyclic cells, which transform into slender bloodstream forms and undergo binary fission to multiply [2,4,5]. They then differentiate into non-replicative stumpy forms. Stumpy cells then re-enter the insect vector *via* bloodmeal after which they undergo a transformation into the procyclic

stage in the digestive tract of the insect and regain the ability to divide. Further differentiation into metacyclic forms occurs and they subsequently differentiate into epimastigotes after moving to the tsetse fly salivary gland, where the cells divide and form metacyclic cells able to infect mammals [2,4].

T. brucei has a distinct cellular morphology. Although significant morphological changes take place during the life cycle, the parasite generally exhibits an elongated shape, maintained by sub-pellicular microtubules within the cell. The flagellum, enabling movement of the cell in its host environment, is situated along the exterior cell membrane and exits at the flagellar pocket where it is connected to the basal body. The kinetoplast DNA, found in the elongated unique mitochondrion of the cell is linked to the basal body through the tripartite attachment complex. Additionally, glycosomes, organelles taking part in the energy metabolism, are found in the cytoplasm, as well as the nucleus, bearing the genomic DNA. The sole Golgi apparatus of the cell is situated next to the nucleus and the flagellar pocket [2].

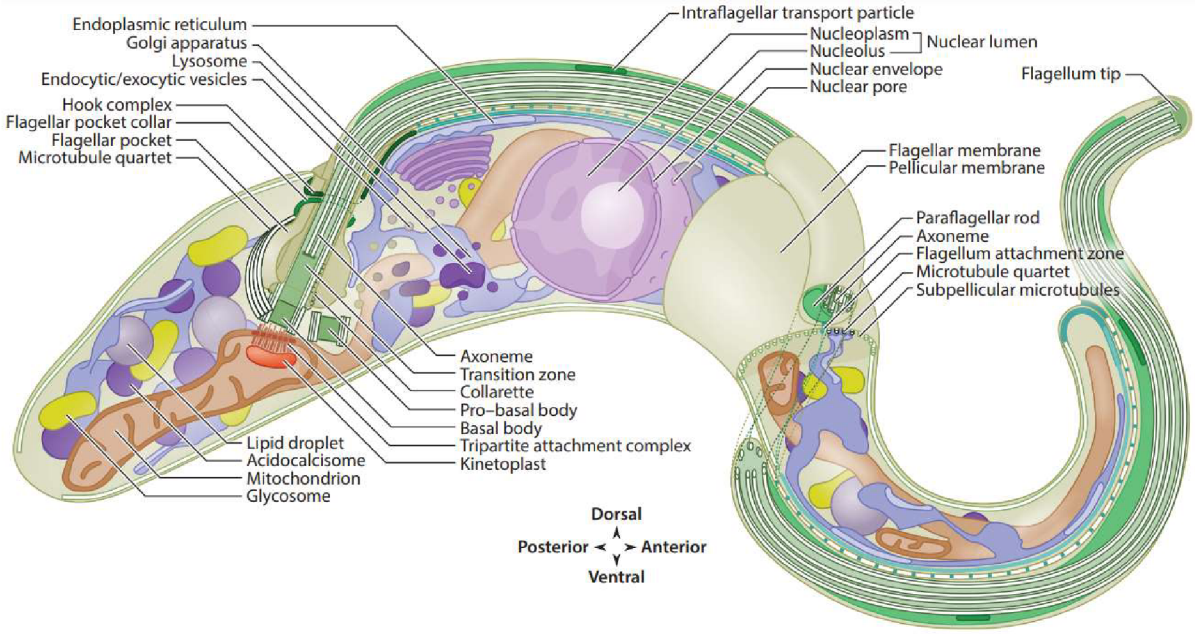

Figure 2: Schematic representation of *T. brucei* cellular organization [6]

1.2 Cellular specializations of *T. brucei*

The two main stages of the life cycle, the procyclic and bloodstream forms of the parasite, display cellular specializations as many other protozoan parasites like *Trypanosoma cruzi* and *Leishmania mexicana* do, amongst which both the cytostome-cytopharynx complex, involved

in endocytosis, and the megasome, a cytoplasmic organelle with lysosomal characteristics, can be mentioned respectively [7].

Depending on the life cycle stage, *T. brucei* cells are known to produce ATP by different ways: Procyclics generate it mainly through oxidative phosphorylation, while bloodstream cells rely on glycolysis to cover their energetic needs [8]. The glycosome is essential for the execution of this process and several organisms belonging to the Kinetoplastida class, including *T. brucei*, contain it. This organelle shares characteristics with peroxisomes such as the absence of organellar DNA, being enclosed by a single organellar membrane and undergoing fission during replication. Glycosomes almost exclusively contain proteins needed for glycolysis when examined in the *T. brucei* bloodstream form. In contrast, less than half of glycosomal enzymes found in procyclic parasites are connected to the glycolytic pathway [9,10].

While the *T. brucei* genome is organized in 11 major and various minor chromosomes in the cell nucleus, the DNA of the sole mitochondrion is organized in 25 maxicircles, in which the information for 18 genes associated with oxidative phosphorylation, and the code for the ribosomal subunits found in the mitochondrial organelle is stored [11–14]. Additionally, estimated 5000 minicircles, coding for guide RNAs needed for modifications of RNA sequences *via* RNA editing, can also be found and, together with the maxicircles constitute the so-called kinetoplast DNA [13,14]. The architecture and activity of the mitochondrion changes through the parasite's life cycle. Mitochondria found in the bloodstream form cells have a tubular structure and do not produce energy through oxidative phosphorylation. Nonetheless, tube-like cristae, which are replicated during cell division, constitute approximately 2% of the organellar volume. Contrarily, the sizable procyclic mitochondrion performs oxidative phosphorylation for ATP production and has disk-shaped cristae that highly vary in size and occupy four times more volume compared to the cristae in bloodstream form cells [13,15].

Accurate division and subsequent distribution of this organelle to daughter cells, together with the kinetoplast DNA is critical. This separation is mediated by the basal bodies, in a concerted process attached to the kinetoplast *via* the tripartite attachment complex [13].

1.3 The tripartite attachment complex

The TAC divides the multiplied kinetoplast DNA during replication and consists of three distinct units with, in total, 13 known associated proteins: the exclusion zone filaments, the differentiated membranes of the mitochondrion and the unilateral filaments [16,17]. Through the exclusion zone filaments, which do not contain ribosomes, the flagellar basal body is joined with the exterior of the mitochondrial membrane. The unilateral filaments attach the interior of the mitochondrial membrane to the kinetoplast DNA, with the area next to the kinetoplast being DNA-rich and having a high pH with the opposite occurring adjacent to the organellar membrane. At the same time as the cell division the TAC is constructed *de novo* from the flagellar basal body in direction to the kinetoplast [16–18]. Additionally, through connecting the basal body with the organellar membrane, the mitochondrion is held in place next to the flagellum during kinetoplast DNA replication by the TAC exclusion zone filaments [16].

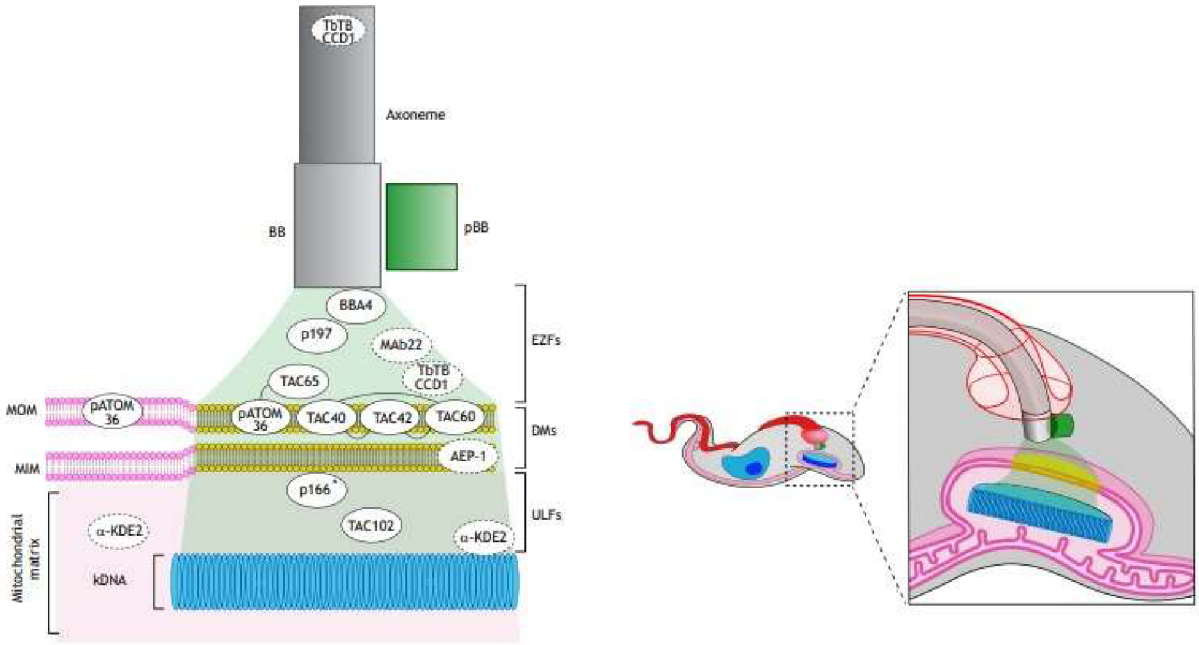

Figure 3: Structure of the TAC, its associated proteins and position within the *T. brucei* cell (adapted from [18]). EZFs, DMs and ULFs stand for exclusion zone filaments, differential membranes, and unilateral filaments respectively. Both the DNA found in the nucleus and the kinetoplast DNA are blue, the mitochondrial organellar membrane is pink outside and yellow within the TAC and the basal body (BB) has a grey coloration. The probasal body (pBB) is green. MOM and MIM stand for mitochondrial outer and mitochondrial inner membrane respectively [18].

Proteins associated with the exclusion zone filaments are: BBA4, p197, MAb22, TAC65 and TbTBCCD1. The proteins connected with the mitochondrial membrane at the position of the TAC are pATOM36, TAC40, TAC42, TAC60 and AEP-1, while TAC102, α-KDE2 and p166 are linked to the unilateral filaments [18].

The importance of the identification of novel TAC proteins relies in its significance in the *T. brucei* cell cycle and was addressed by Baudouin et al. using different approaches [17].

1.4 TriTryp and TrypTag databases

To facilitate the research of trypanosomatids, including *T. brucei*, a centralized online database was created in the year 2010, the so called TriTrypDB. This resource enables the visualization and curation of scientific data derived from fully sequenced genomes, proteomes and transcriptomes, among others, on one website (tritrypdb.org) [19].

Another valuable resource available online, the TrypTag database (tryptag.org), provides information about the localization of a vast number of *T. brucei* proteins within the parasitic cell, excluding post-translationally modified proteins and surface polypeptides, and a final number of 15297 proteins upon completion, to aid in the research regarding their function and association with specific cellular organelles [20]. As of 2017, four out of ten coding genes found in the fully sequenced *T. brucei* genome encode presumed proteins, with only scarce if any knowledge regarding their functions available [20,21]. Briefly, TrypTag methodology consists in endogenous gene-tagging at the protein termini, using the fluorescent mNeonGreen tag, and visualization of the tagged products by automated fluorescence microscopy. Proteins with known targeting signals, which usually are located at the N-terminus, are only tagged at the C-terminus, while with remaining protein types tagging is applied at both termini [20].

The proteins examined, namely Tb927.11.13600, Tb.927.11.14570, Tb927.4.840 and Tb927.6.4540, called Tb13600, Tb14570, Tb840 and Tb4540 in this thesis, all exhibited a TAC relation according to their TrypTag C-terminal tagging results, while N-terminal tagging, when successfully conducted, displayed a cytoplasmic localization, suggesting possible N-terminal TAC targeting signals [20]. However, relations to the mitochondrion itself or the kinetoplast were also found and the mNeonGreen tag used is known to alter the physiological topology, which may cause artifacts [20,22]. Therefore, the exact localization of the proteins was assessed further through IFA and WB analysis with a distinct 3xV5 C-terminal tag. Additionally, RNAi was conducted to examine the essentiality of these proteins.

2 Aims

The aims of this thesis were to validate the TrypTag observed "TAC-like" localization of the proteins Tb927.11.13600, Tb927.11.14570, Tb927.4.840 and Tb927.6.4540 in the procyclic form of *T. brucei* organism using endogenous *in-situ* tagging and, subsequent western blotting and IFA analysis. Additionally, we examined the essentiality of these proteins by the generation of RNAi knockdown strains of *T. brucei* procyclics and evaluating the effects on growth.

3 Material and Methods

3.1 Cell cultures

All experiments involving parasitic cells were conducted using SmOxP427 cell line cells, procyclic Lister 427 *T. brucei* parasites previously transfected with the SmOx plasmid, which is integrated between tubulin loci. The linearized SmOx vector consists of a T7 RNA polymerase gene, a tetracycline repressor and puromycin resistance gene. Therefore, SmOx cell lines enable Tet inducible expression of genes [23].

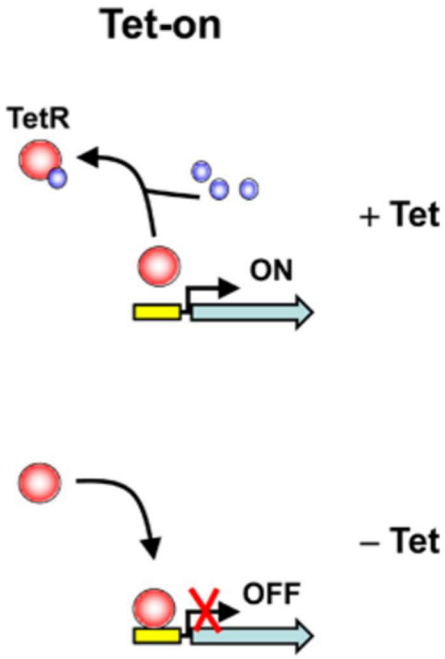

Figure 4: Scheme of the tetracycline inducible expression of a gene in a so-called Tet-on system [24]. The addition of the antibiotic leads to the transcription of the gene insert. In contrast, without adding tetracycline no expression takes place.

T. brucei procyclic forms were grown at 27 °C in 25 cm^3 tissue culture flasks containing SDM-79 medium supplemented with 10% FBS and the antibiotics necessary for selection, with the final concentrations of 50 µg/mL and 1 µg/mL for hygromycin, used after tagging transfection, and puromycin, used after RNAi plasmid transfection, from stock solutions of 50 mg/mL and 1 mg/mL (1:1000), respectively.

The cultures were diluted regularly every two days to keep the cells exponentially growing and prevent cell death due to hyperacidity and exhaustion of the culture medium. This was done by replacing four fifths of the culture with fresh medium containing antibiotics, thereby maintaining cell densities amid $1 \cdot 10^6$ to $1 \cdot 10^7$ cells/mL.

Table 1: Composition of SDM-79 medium with 10 % FBS (1 L)

Reagent	Amount
SDM-79 powder	25.5 g
Hemin (2.5 mg/mL)	3 mL
Penicillin-streptomycin 100x (1000 U/mL, Sigma)	10 mL
FBS (10% V/V)	100 mL
Milli-Q water (to final volume of 1000 mL)	887 mL

3.2 PCR dependent techniques

3.2.1 Generation of *in-situ* tagging constructs

In-situ tagging at the C-terminus of the prioritized proteins was achieved by long primer PCR using the pPOTv5 plasmid as template, a modified pPOTv4 plasmid containing a 3xV5 tag sequence instead of a YFP-tag and a hygromycin antibiotic resistance gene. This method requires the design of forward primers consisting of 80 bp coding sequence upstream to the annotated stop codon and excluding it, plus 18 additional nucleotides coding for a region corresponding to the pPOT plasmid used, to enable annealing to the vector during PCR. The reverse primers consist of the initial 80 bps downstream from the annotated stop codon and excluding it, plus a 20 bp sequence annealing to the plasmid sequence [25]. After PCR of the tagging products, the expected size was verified by agarose gel and the PCR reactions were used for transfections. Figure 5 depicts schematically how the PCR product was generated and the recombination event in the genome after transfection.

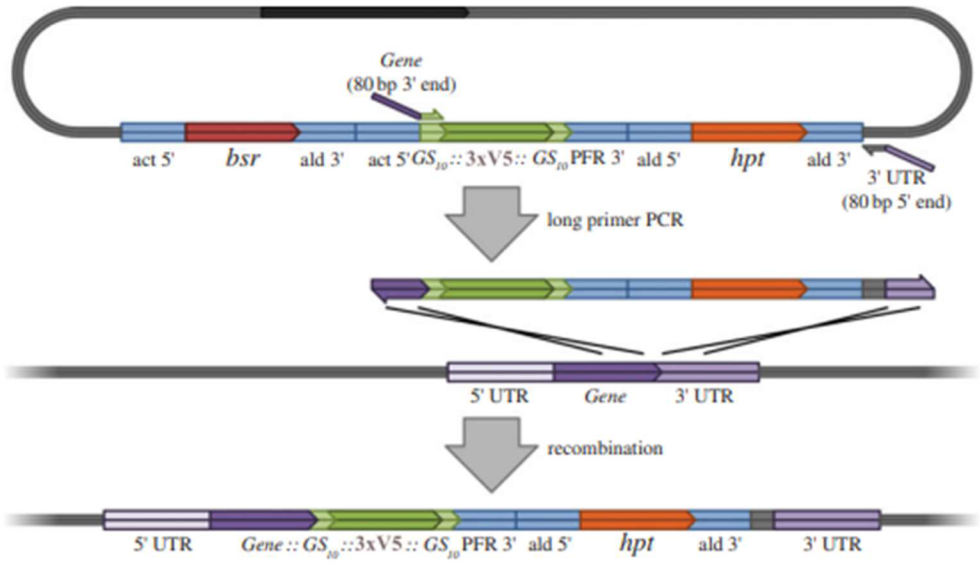

Figure 5: Scheme showing an example of tagging at the C-terminus with the PCR generated tagging construct. act is an actin UTR, bsr an blastidicin resistance gene, ald an aldolase UTR, GS_{10} a primer binding site accommodating a glycine-serine linker, 3xV5 the tagging epitope, PFR an UTR of the paraflagellar rod protein and hpt the hygromycin resistance gene. After

transfection of the long primer PCR product (first vertical arrow) and homologous recombination (second vertical arrow), an in frame 3xV5 tag is added to the 3' end of one allele of the gene of interest, that is later expressed as a translational fusion (not shown, modified from [25]).

Table 2: Long primer PCR mix composition for one reaction

Reagent	Amount
Q5 polymerase 2x mix (NEB)	25 µL
Milli-Q water (to a final volume of 50 µL)	23 µL
Forward primer (20 µM)	1 µL
Reverse primer (20 µM)	1 µL
pPOTv5 vector (template)	less than 0.5 µL

Table 3: Conditions for long primer PCR

Step	Temperature	Time	Cycles
Preheating	98 °C	2 minutes	1
Denaturation	98 °C	20 seconds	15
Gradient annealing step	65 to 50 °C (decreased by -1 °C per cycle)	30 seconds	
Extension	72 °C	2 minutes	
Denaturation	98 °C	20 seconds	20
Annealing	50 °C	30 seconds	
Extension	72 °C	2 minutes	
Final extension	72 °C	2 minutes	1
Hold temperature	4 °C	infinite	1

Table 4: Primer sequences for tagging amplicon. Sequences annealing to the pPOT vector are shown in red, 80 bp gene specific sequences annealing to 3' coding DNA sequence and 3' UTR are shown in black

Primer	Sequence
Tb13600 forward	ACCATAACGATAAGAAGGGTAGGAGCAGCAGGGAAAGG GGAAATGCAGGCGGAAGGCACGAGTCCAGACGGCGGCA GCGCGGTTCTGGTAGTGGTTCC
Tb13600 reverse	AAGAGGGAGGGAGAGGAGCTAGTTGAGAACAAACCCGA TCATGAGATTGTGAGGAGGCCTCTGACACCAGTTGGTTA GCGCCAATTTGAGAGACCTGTGC
Tb14570 forward	GTAAGGATTGGCGCACCCCGCGGCGGTTCACGTATGCAG AGGGGTTACAAAATGGAGGCTTTGCAAATATCATTGACG AGGGTTCTGGTAGTGGTTCC
Tb14570 reverse	TTCTACTTTTTCTTGCCTGTTAGCTTAGTGCCGCTTCTGGT TAAACTACTTGGTGCACCTAGCACCGCATTATCGTGATG CCAATTTGAGAGACCTGTGC
Tb840 forward	CGGGAAGCGGCACAACCGTTCGTGTAACTTTTCCAAAAG CTCCAGTAGAGGTGCTTTTGCCTGAGATGAGTGCGCCGT GGGGTTCTGGTAGTGGTTCC
Tb840 reverse	ACTGCCACGGAATGGGCACGCCTTGACGCGTTTTGCCCA CAACATAATTGAAGCTCCTCCTTCCTCCTCCTCTCTTTCC ACCAATTTGAGAGACCTGTGC

Tb4540 forward	TTTCTGCGGAACTGTCGCTCATGTCAGGGTTGGCTGCAG GGCACCTCCTAAGTGCCCACATGCGGTTGAATCGTAGGA AGGGTTCTGGTAGTGGTTCC
Tb4540 reverse	CCCTTGTGCAACCCACAAGGACAACGCACATTGCCCTCT CCACCACACTCTACTTCATACTGGTTTCATTTTTATCCGC ACCAATTTGAGAGACCTGTGC

3.2.2 RNAi gene silencing and Gibson assembly of RNAi constructs

RNAi is a process that allows the genetic knockdown of targeted genes in eukaryotic organisms, including *T. brucei* [26,27]. Initially, transcribed double stranded RNA sequences involved in gene silencing, which either form stem-loop structures or linear double-strands, undergo post-transcriptional splicing and subsequent export to the cytoplasm, where they are enzymatically cleaved by the Dicer nuclease into 22 bp long double stranded RNA fragments. The double stranded fragments are then transported into the RISC and the strands are separated. One of these single strands then conjugates to the transcribed messenger RNA sequence of the targeted gene. Depending on the locus of conjugation and if the fragment is a complete match to the messenger RNA the targeted sequence is either cut and disassembled or prevented from undergoing translation, leading both to RNAi mediated knockdown [26].

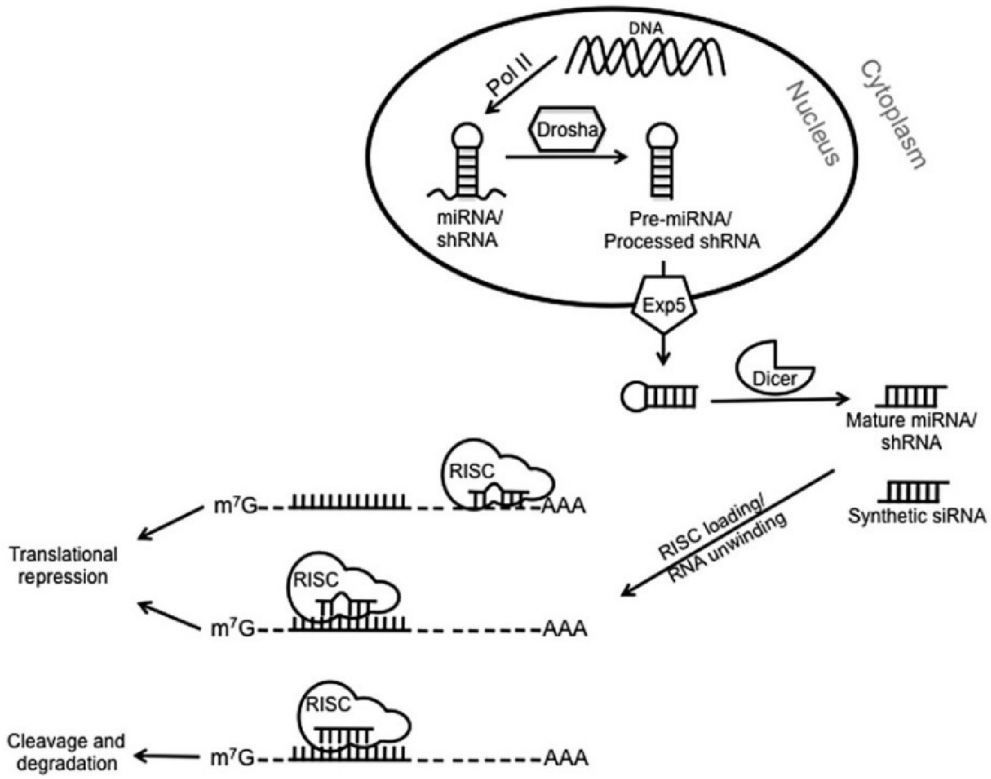

Figure 6: Illustration of the RNAi mechanism. Pol II stands for the RNA polymerase II which transcribes the sequence, drosha is the enzyme that post-transcriptionally splices the generated hairpin, miRNA and shRNA stand for microRNA and small hairpin RNA respectively [26]

RNAi constructs for the generation of RNAi hairpins were constructed by Gibson assembly, which is a method that enables the end to end joining of distinct DNA fragments. Each fragment contains homologous overhangs. These identical sequences enable the joining of the sections by removing the nucleotides in the 5'-3' direction using 5' exonuclease. Then the resulting overlaps are annealed to their complement and DNA polymerase and DNA ligase are applied to reestablish double strands by replacing the nucleotides, leading to the assembly of the new DNA molecule.[27,28]. Figure 7 depicts the steps of a Gibson assembly reaction.

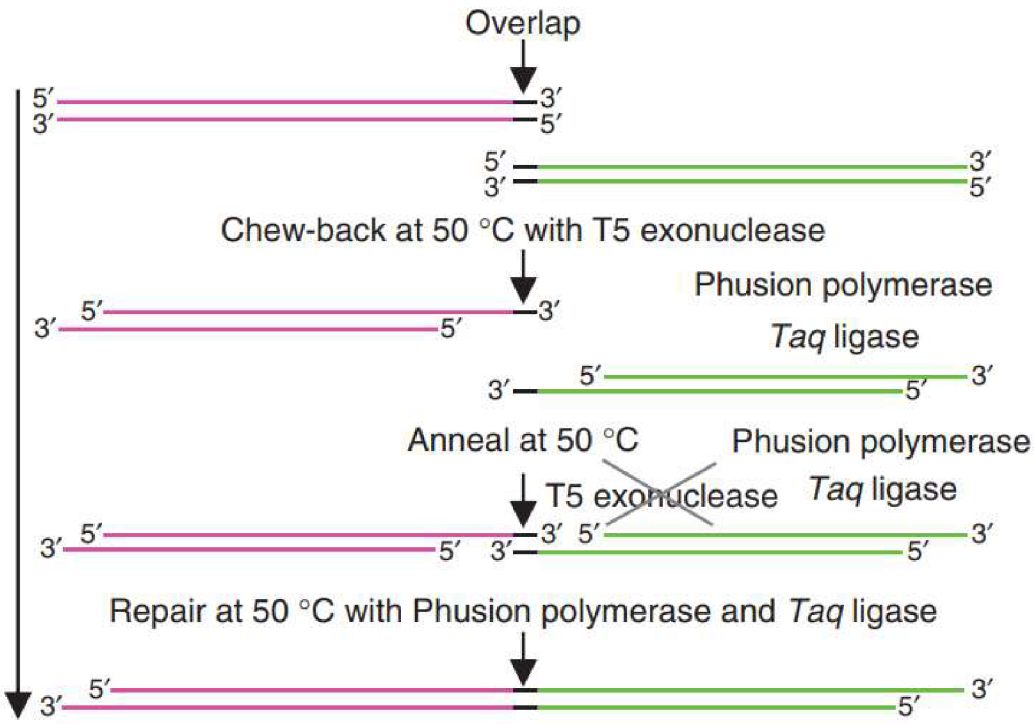

Figure 7: Gibson assembly scheme, depicting the procedure as stated above [28]

To generate RNAi induced genetic knockdown cell lines, lhRNAi constructs were assembled *via* Gibson assembly with the pTrypson vector as a backbone [27,28]. Hairpin RNA is a single stranded RNA fragment that conjugates complementary parts of its sequence, leading to a stem-loop form [27]. It has advantages over RNAi that employs linear double stranded RNA due to more efficient gene knockdown and an avoidance of a host immune response [27,29]. The RNAi constructs in the pTrypson plasmid are composed of a stuffer bordered by the gene targeted by RNAi on both sides and the pTrypson backbone. In between the stuffer and gene sequence and between the gene and the plasmid backbone, restriction sites for the enzymes XhoI and HindIII are situated respectively [27].

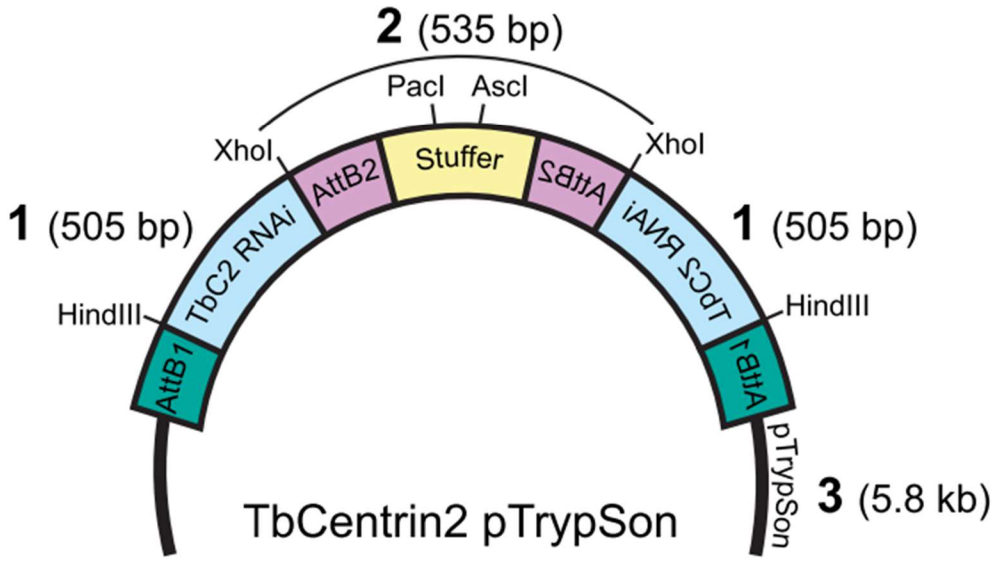

Figure 8: Scheme of a pTrypson plasmid example containing TbCentrin2 (TbC2 RNAi) gene inserts for RNAi. The homologous gene inserts in turquoise with 505 bp length (1) are flanked by AttB1 and AttB2 sections in green and purple and contain restriction sites for XhoI and HindIII on one side each respectively. The stuffer in orange with PacI and AscI restriction sites with a length of 535 bp when combined with two AttB2 sections (2) is situated between the inverted repeats of the gene insert. The AttB1 sequences are connected *via* the 5.8 kb plasmid backbone (3) [27].

Primers specific for the gene of interest with overhangs and sequences corresponding to the AttB1 and AttB2 regions situated in the stuffer and backbone sequences were created and used during PCR with *T. brucei* TREU 927/4 gDNA as a template. The correct amplification and size of the desired fragments was examined by performing an agarose gel electrophoresis. PCR products were purified using a clean-up kit (MinElute PCR Purification Kit, Qiagen) by binding the DNA to a silica membrane in an environment with elevated salt levels and a slightly acidic pH, enabling the purification using buffer solutions followed by elution with Milli-Q water [30]. To purify the DNA the PCR product was pH adjusted until the mixture showed a yellow coloration. Then the liquid was transferred to a column within a test tube and centrifuged at 13000 rpm for 1 minute, followed by removal of the flow through. 750 µL PE buffer were added and the column centrifuged twice for 1 minute, each time discarding the flow through. After transfer to a new test tube the sample was eluted by the addition of 10 µL Milli-Q water and centrifuged for 1 minute after a 1-minute waiting time. Gibson assembly was performed at 50 °C for three hours by combining the plasmid components, namely the vector backbone, the PCR generated stuffer and the PCR reaction corresponding to the genes of interest, with a 2x Gibson assembly master mix. The generation of the stuffer and the plasmid backbone, which both were provided, were conducted with primers corresponding to the AttB2 region and the same PCR conditions as mentioned earlier, using the pTrypson vector as a template, and HindIII restriction digestion of the plasmid respectively. The 150 ng PCR product containing the gene of interest were added after previous quantification using

NanoDrop (Thermo Scientific) and subsequent adjustment of the volume to follow the manufacturer's specifications.

Table 5: RNAi PCR mix composition for one reaction

Reagent	Amount
Q5 polymerase 2x mix (NEB)	25 µL
Milli-Q water (to a final volume of 50 µL)	22 µL
Forward primer (20 µM)	1 µL
Reverse primer (20 µM)	1 µL
gDNA *T. brucei* TREU 927/4	1 µL

Table 6: Conditions for RNAi PCR

Step	Temperature	Time	Cycles
Preheating	98 °C	2 minutes	1
Denaturation	98 °C	20 seconds	15
Gradient annealing step	65 to 50 °C (decreased by -1 °C per cycle)	30 seconds	
Extension	72 °C	2 minutes	
Denaturation	98 °C	20 seconds	20
Annealing	50 °C	30 seconds	
Extension	72 °C	2 minutes	
Final extension	72 °C	2 minutes	1
Hold temperature	4 °C	infinite	1

Table 7: Gibson assembly mix composition for one reaction

Reagent	Concentration	Amount
Stuffer	200 ng/µL	0.75 µL
pTrypson backbone	500 ng/µL	0.1 µL
Previous RNAi-PCR product	Checked by NanoDrop (varies)	1.5 µL
Milli-Q water (to a final volume of 10 µL)	-	2.65 µL
2x Gibson assembly master mix (NEB)	-	5 µL

Table 8: Primer sequences used for the amplification of the stuffer sequence from the pTrypson vector *via* PCR

Primer	Sequence
Stuffer primer forward	ACCCAGCTTTCTTGTACAAAGTGGTTTGAT
Stuffer primer reverse	ACCCAGCTTTCTTGTACAAAGTGGTTTGAT

Table 9: RNAi PCR primer sequences. Sequences annealing to the gDNA are in red, restriction sites are underlined and wavy for HindIII, straight for XhoI, Gibson assembly overhangs are grey

Primer	Sequence
Tb13600 forward	ACAAGTTTGTACAAAAAAGCAGGCTAAGCTTGGTGGCC AGACTCGAAAGAA
Tb13600 reverse	ACCACTTTGTACAAGAAAGCTGGGTCTCGAGCCTGCATT TCCCCTTTCCCT
Tb14570 forward	ACAAGTTTGTACAAAAAAGCAGGCTAAGCTTTTCAACAA TGTTGGCAGGCG
Tb14570 reverse	ACCACTTTGTACAAGAAAGCTGGGTCTCGAGAGGGCGG CATGTGACAATAA
Tb840 forward	ACAAGTTTGTACAAAAAAGCAGGCTAAGCTTAGCAACC GGAGAGTGACAAG
Tb840 reverse	ACCACTTTGTACAAGAAAGCTGGGTCTCGAGTACGCAAG GTGTCCCTCAAC
Tb4540 forward	ACAAGTTTGTACAAAAAAGCAGGCTAAGCTTCTTGTGGG ACAGGCAAAACG
Tb4540 reverse	ACCACTTTGTACAAGAAAGCTGGGTCTCGAGGCTTTGCG ACCGATGATGAC

3.2.3 Transformation in *E. coli* and colony PCR screening

Transformation is the process of introducing external DNA into a bacterial organism through permeation of the cell membrane. *E. coli* previously treated with $CaCl_2$, which increases the permeability, is stimulated to take up a foreign plasmid by rapidly increasing and decreasing the surrounding temperature *via* heat shock and subsequent cooling on ice [31,32]. The plasmid contains a gene encoding for an antibiotic resistance, typically and in our case ampicillin, allowing selection of bacteria that bear the plasmid after transfection [31]. After plating the transformation reaction on agar plates, colonies can be visualized, each of them representing one bacterial clone. Screening of these clones or colonies using Colony PCR is performed to confirm the incorporation of the desired plasmid into the bacteria. To that end, a sequence is amplified from the plasmid in the bacterial colony by PCR using specific primers [33].

A transformation of the pTrypson vectors bearing RNAi constructs previously generated through Gibson assembly into *E. coli* XL 1-blue strain was performed by the addition of 50 µL of competent bacteria to 3 µL aliquots of the Gibson assembly reaction each. After 30 minutes of incubation on ice a heat shock at 42 °C for 40 seconds was conducted. Subsequently, the mixes were put on ice for 5 additional minutes and thereafter added to 1 mL LB media. After 1 hour of incubation at 37 °C the samples underwent centrifugation for 10

minutes at 3000 rpm. 800 µL of the resulting supernatants were discarded while the pellets were resuspended in the remaining 200 µL of LB media, which then was used for inoculation on ampicillin containing agar Petri dishes. After incubation at 37 °C overnight colony PCRs were conducted to verify the presence of the desired plasmid.

Colony PCR was performed by removing the chosen bacterial colonies, inoculating a new control agar plate and transferring the remaining bacteria in a pipette tip to a tube containing 8 µL of Milli-Q water followed by resuspension and cell lysis using the thermocycler. Then the respective pre-prepared mix (Table 10) was added to the solution and PCR over the gene of interest was performed using the respective forward gene specific primer from the initial generation of the RNAi gene insert and a gRNAi SEQ reverse primer specific to the stuffer present in the vector backbone. This was followed by agarose gel electrophoresis for visualization and verification of the correctly sized products according to their expected size.

Table 10: Colony PCR mix composition for one reaction

Reagent	Amount
2x ToppBioPPP Master Mix	10 µL
Milli-Q water	8 µL
RNAi gene specific forward primer	1 µL
gRNAi SEQ reverse primer (stuffer)	1 µL

Table 11: Cell lysis program

Temperature	Time
96 °C	5 minutes
50 °C	1 minute 50 seconds
96 °C	1 minute 50 seconds
45 °C	1 minute
96 °C	1 minute
40 °C	1 minute
4 °C	2 minutes

Table 12: Conditions for colony PCR

Step	Temperature	Time	Cycles
Preheating	94 °C	2 minutes	1
Denaturation	94 °C	20 seconds	15
Gradient annealing step	65 °C to 50 °C (decreased by -1 °C per cycle)	30 seconds	
Extension	72 °C	1 minute 15 seconds	
Denaturation	94 °C	20 seconds	20
Annealing	50 °C	30 seconds	
Extension	72 °C	1 minute 15 seconds	
Final extension	72 °C	7 minutes	1
Hold temperature	12 °C	12 minutes	1

Table 13: gRNAi SEQ primer sequences

Primer	Sequence
gRNAi SEQ forward	CGCTGACTTTCCAAGACCTC
gRNAi SEQ reverse	CAGATCGTCTTCACCCCCTA

After verification, colonies bearing the correct RNAi constructs were amplified in 5 mL LB media containing ampicillin with a final concentration of 50 µg/mL at 37 °C overnight. Following centrifugation at 3000 rpm for 10 minutes the plasmids were extracted from the resulting pellets using a Miniprep kit (Hybrid-Q Plasmid Rapidprep Kit, GeneAll). The principle of this kit consists of two steps. Firstly, RNA is eliminated by RNAse present in solution S1. The cell membrane is disrupted and protein structures are destabilized by SDS, while DNA strands are separated by NaOH *via* the addition of the second solution. Neutralization using solution 3 follows to allow binding to microfibers in an environment with increased salt concentrations and the subsequent removal of unwanted substances like genomic DNA. Miniprep was conducted by adding 250 µL S1 buffer to the pellets, followed by resuspension and relocation of the solution to a test tube. After addition of 250 µL S2 buffer and 350 µL G3 buffer, followed by mixing through gentle repeated inversion after each step respectively and 10 minutes of centrifugation. The resulting supernatant was added to a spin-column. Centrifugation for 30 seconds was followed by removal of the flow-through and 700 µL PW buffer. After two rounds of centrifugation for 30 seconds and 1 minute each and the removal of the resulting flow through and the transport of the spin-column to a new test tube 50 µL Milli-Q water were added. 1 minute later centrifugation for 1 minute was conducted, finalizing the process. Each centrifugation was performed with 14000 rpm [34].

The extracted plasmid DNA was then used for an additional check for correct plasmid composition by cutting the restriction sites using XhoI and HindIII-Hf and incubating the samples at 37 °C for one hour. Furthermore, the samples were sent for sequencing. After sequencing, plasmid DNA was prepared for transfection through digestion with the restriction enzyme NotI-Hf followed by PCR clean-up (MinElute PCR Purification Kit, Qiagen) to linearize the plasmid prior to transfection to enable correct recombination into the *T. brucei* genome.

Table 14: Restriction check mix composition for one reaction

Reagent	Amount
Cutsmart (NEB)	1 µL
XhoI	0.2 µL
HindIII-Hf	0.2 µL
Plasmid DNA sample	2 µL
Milli-Q water (to a final volume of 10 µL)	6.6 µL

3.3 Transfection

Transfection enables the insertion of external DNA into a eukaryotic genome, resulting in the expression of the transfected genetic material. Foreign DNA can be introduced into a cell *via* three method types that are based on chemicals, biological approaches and the alteration of the physical environment respectively. An example for the application of chemicals is calcium phosphate, which forms complexes in the presence of DNA that traverse the cellular and nuclear membranes, leading to the transfection of the external DNA. Biological vectors like viruses transduce external DNA, that replaced pathogenic viral genes in the genome through previous interventions, by infecting the cell [35]. An example for a physical approach is electroporation, which leads to the generation of pores in the cell membrane by disrupting the plasma membrane using electric pulses, allowing the translocation of foreign DNA into the cell [35,36]. During this thesis transfections were performed using the AMAXA Nucleofector II VPA-1002 device (Lonza Bioscience) which inserts previously linearized plasmid DNA into *T. brucei* procyclic cells through electroporation [37].

Firstly, $5 \cdot 10^7$ cells in mid-log growth were collected and centrifuged at 1300 rcf at 4 °C for 10 minutes and the supernatant discarded. After resuspension in 100 µL transfection buffer consisting out of 81.8 µL human T-cell Nucleofector solution and 18.2 µL supplement 1 to which 10 µL of previously prepared DNA to be transfected were added the mixture was transferred into a glass cuvette with a 2 mm gap. Subsequently, electroporation by giving one pulse using the AMAXA Nucleofector II machine and its X-014 program was performed. Afterwards the electroporated mixture was added to 6 mL SDM-79 10% FBS medium without antibiotics and kept at 27 °C for 16-18 hours. Then the cell suspension was brought to a final volume of 12 mL with 6 mL of growth medium containg 2x the concentration of the relevant antibiotic (hygromycin for tagged cell lines, phleomycin for RNAi cell lines, with concentrations of 50 µg/mL and 1 µg/mL respectively). Subsequent selection for semi-clonal *T. brucei* populations was conducted by adding serial dilution as follows: First, 1.5 mL of fresh medium with antibiotic were added to the second and third row and 1 mL to the fourth row of a 24-well plate. The wells of the first row then were then supplemented with 2 mL of cell containing media. After thorough mixing 0.5 ml were removed from each well and transferred to a well in the second row. This step was repeated two more times, performing a 1:3 serial dilution and leading to a final volume of 1.5 mL in each well of the 24-well plate. A control cell line was set up by performing transfection without the introduction of foreign DNA in the

process. Transfection progress was monitored daily. After 10 days and the death of the control cell line positive wells showing growing cells were transferred to 25 cm^3 tissue culture flasks and further propagated in 5 mL SDM-79 media with 10% FBS and appropriate antibiotics. One clone was evaluated each either for expression of 3xV5-tagged products or for standard growth curves and RNAi protein knockdown.

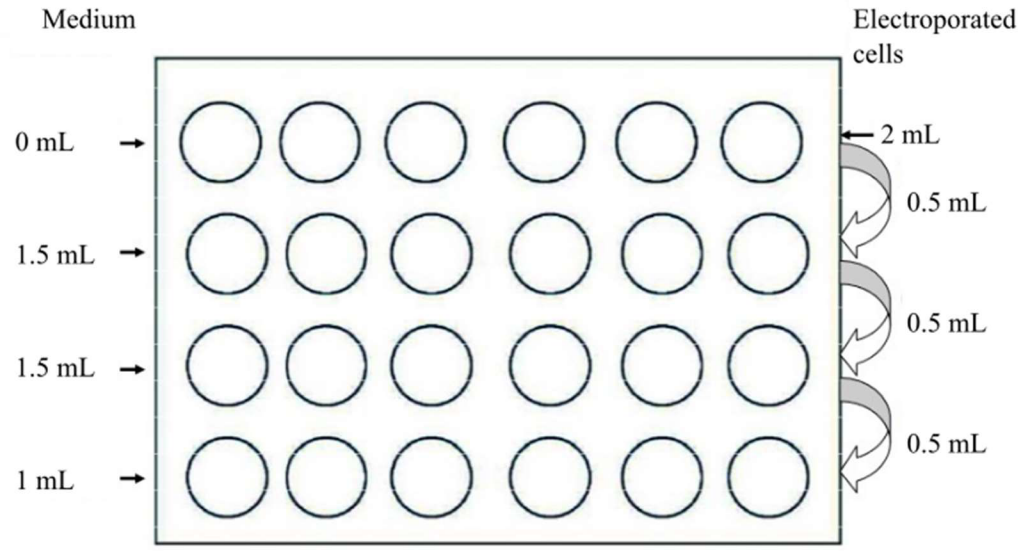

Figure 9: Serial dilution procedure for the selection of semi-clonal populations after electroporation. After the addition of 1.5 mL of fresh media to the second and third row and 1 mL to the fourth row 2 mL of culture containing electroporated cells are added to the first row. The arrows indicate the subsequent transfer of 0.5 mL from the first row to the second and so on to achieve a 1:3 serial dilution (modified from [38])

3.4 Agarose gel electrophoresis

Agarose gel electrophoresis was performed to confirm the size of the PCR products and restriction digests through DNA separation. The gel forms pores with certain diameters which delay the flow of DNA samples based on size, thus separating them. Larger DNA fragments have a longer migration time and pore size depends on the agarose concentration of the gel. All DNA has a negative charge due to its phosphate backbone and under influence of an electric field always migrates towards the anode. Ethidium bromide, which binds to the DNA and exhibits fluorescence under UV light, is used to visualize the DNA fragments [39].

An 1% agarose gel was prepared by dissolving 0.8 g of agarose in 80 mL TAE buffer through heating in a microwave oven until boiling. The resulting solution was then cooled 5 µL ethidium bromide were added. Then the mixture was poured into an appropriate cast with a comb and left to jellify for 20 minutes. Subsequently, the gel was submerged in 1.5 L of a

TAE buffer solution. After removal of the comb the resulting wells were filled with 5 µL sample previously mixed with 1 µL loading dye leading to a total sample volume of 6 µL. An empty well was loaded with 5 µL of DNA-ladder. The electrophoresis was conducted at 110 V for 45 minutes and visualized under UV light using a ChemiDoc (Bio-Rad) apparatus.

3.5 WB analysis

WB analyses were conducted over whole cell lysates to confirm the correct tagging of the proteins of interest with the 3xV5 epitope after transfection. Subsequent crude cellular fractionations of the whole cell lysate then allowed for the subcellular localization analyses of the tagged proteins.

3.5.1 Sample preparation for WB analysis

Whole cell lysate samples were prepared by harvesting $5 \cdot 10^6$ cells, which were centrifuged at 900 x g for 3 minutes. After removal of the supernatant the pellet was washed twice in 1 mL PBS. Subsequently, the pellet was resuspended in 40 µL PBS and 40 µL 2x Laemmli buffer. The cell suspension was heated to 95 °C for 5 minutes. 10 µL were used to perform an SDS-PAGE, followed by a WB.

To analyze the subcellular distribution of the proteins of interest a digitonin based crude cellular fractionation was conducted. Digitonin interacts with cholesterol and leads to the rupture of membranes with high cholesterol amounts, like the cell membrane, while leaving the organellar membranes, which contain smaller quantities of cholesterol, intact at low concentrations [40,41].

Cells from 4 mL of culture were harvested *via* centrifugation at 1000 x g and 4 °C for 10 minutes. The resulting pellet was washed twice with PBS after the removal of the supernatant and resuspended using 500 µL lysis buffer, which was put on ice earlier. To 400 µL of the suspension 16 µL digitonin were added for a final concentration of 0.4 mg/mL while the remaining 100 µL cell suspension were reserved as the whole cell lysate sample. The digitonin containing fraction was centrifuged at 14,000 x g for 2 minutes at RT. The resulting supernatant was collected and saved as the cytoplasmic sample. Then the mitochondrial fraction was prepared by washing the pellet in lysis buffer once, followed by resuspension in

400 µL lysis buffer. Lastly, 4 µL Triton-X-100 were added for a final concentration of 0.1%. 5 µL 2x Laemmli buffer were added to 15 µL aliquots of each fraction, and an SDS-PAGE and subsequent immunoblotting were performed.

Table 15: Solutions used during sample preparations and their compositions

Reagent	Components	Concentration
Lysis buffer (used in crude subcellular fractionation)	TRIS-HCl	25 mM (pH = 7.6)
	Sucrose	225 mM
	EDTA	2 mM
	EGTA	2 mM
	KH_2PO_4	10 mM
	$MgSO_4$	1 mM
	Sodium-citrate	10 mM
	DTT	2 mM
Digitonin (used in crude subcellular fractionation)	Digitonin in Milli-Q water	10 mg/mL
Triton-X-100 (used in crude subcellular fractionation)	TX-100 in Milli-Q water	10%
PBS (used in whole cell lysate sample preparation and crude subcellular fractionation)	NaCl	137 mM
	KCl	2.7 mM
	Na_2HPO_4	10 mM
	KH_2PO_4	1.8 mM
2x Laemmli buffer (used in whole cell lysate sample preparation and crude subcellular fractionation)	TRIS	0.15 M (pH = 6.8)
	glycerol	30%
	SDS	6%
	DTT	0.3 M
	bromophenol blue	0.02%
	Milli-Q water	bring to 50 mL

3.5.2 SDS-PAGE

SDS-PAGE enables protein separation according to their weight and size. SDS is an ionic detergent that attaches to the proteins, unfolds them, and distributes a uniform negative charge over the whole length of the polypeptides. This then allows them to migrate towards the anode when subjected to an electric field. The pore size of the gel depends on the amount of polymerized acrylamide present and determines the speed at which the denatured proteins travel through the gel, separating them according to their size. SDS-PAGE systems that employ two types of gels with varying polyacrylamide content and pH at the same time, namely stacking and resolving gels enable better band resolution later during separation in the resolving gel by concentrating the sample in the stacking gel [42].

The gel used during SDS-PAGE consisted of a resolving and a stacking gel. Firstly, the resolving gel was poured into a pre-assembled cast, covered in 1 mL n-butanol to prevent contact with oxygen, which inhibits the polymerization reaction, and left to harden. After the removal of the alcohol the stacking gel was introduced into the cast and a comb was added. Following polymerization, the gel was covered in running buffer and the comb removed. 20 µL of samples were injected and run alongside 5 µL of marker at 110 V for 60 to 90 minutes.

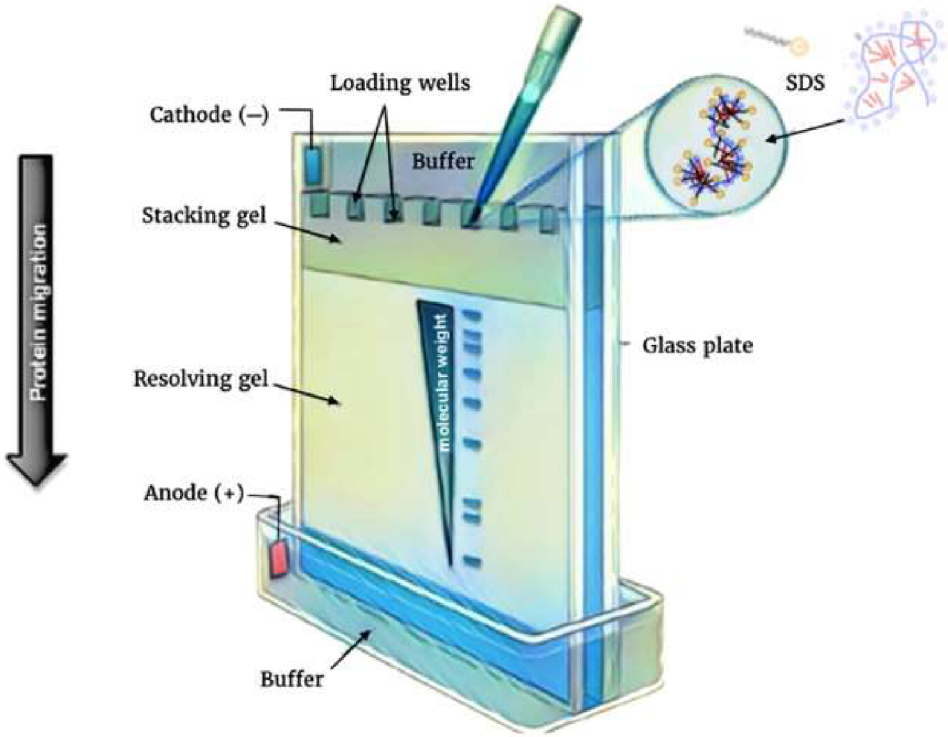

Figure 10: Illustration depicting the mounted system of an SDS-PAGE apparatus consisting of a stacking and a running gel. The black vertical arrow indicates the migration direction of the negatively charged protein samples [43].

Table 16: Compositions of the stacking and running gels for SDS-PAGE

Reagent	12% running gel	5% stacking gel
Milli-Q water	3.3 mL (to 10 mL final volume)	4.38 mL (to 6 mL final volume)
30% acrylamide	4 mL	1 mL
1.5 M TRIS (pH = 8.8)	2.5 mL	-
1 M TRIS (pH = 6.8)	-	0.5 mL
10% SDS	0.1 mL	0.06 mL
APS	0.1 mL	0.06 mL
TEMED	0.004 mL	0.006 mL

Table 17: Running buffer composition

Reagent	Concentration
TRIS	25 mM
glycine	192 mM
SDS	0.1%

3.5.3 Immunoblotting

Immunoblotting is the procedure following SDS-PAGE that allows the visualization of the proteins of interest once they are put in the presence of specific antibodies. In this technique, polypeptides previously separated by SDS-PAGE are transferred to a PVDF membrane using an electric current. It causes the negatively charged proteins to migrate to the anode, thereby bringing about their transfer to the membrane due to its placement in the blotting sandwich. The membrane is then blocked to prevent unspecific interaction of antibodies during the next step, consisting in the specific binding of antibodies to the proteins transferred to the PVDF membrane. While primary antibodies interact specifically with certain epitopes, the secondary antibodies conjugated to HRP bind to the primary antibodies, amplifying the signal and enabling visualization. Following incubation with the antibodies and thorough washing the membrane is developed by treatment with a luminol containing peroxide solution, leading to chemiluminescence [44,45]. This light emission is caused by the interaction of the peroxide with the HRP and the subsequent generation of luminol oxide through an oxidation reaction and leads to the generation of a detectable light emitting compound [45,46].

A PVDF blotting membrane with the dimensions 8 x 7 centimeters was prepared and submerged in methanol, which facilitates the binding of the polypeptides onto the membrane surface by decreasing the membrane hydrophobicity [45]. After assembly in transfer buffer, the blotting sandwich and transfer buffer were transferred to the blotting tank and run at 110 V for 1 hour and 15 minutes. Subsequently, the membrane was blocked using 30 mL 5% milk in PBS-T blocking solution for 1 hour on a rotator. Then the membrane was incubated with 10 mL blocking solution with the primary antibody and kept overnight at 4 °C under rotation. The next day the membrane was washed with 30 mL 0.05% PBS-T five times for 5 minutes each, succeeded by incubation in 10 mL blocking solution containing the secondary antibody for 1 hour. Following five washes with 0.05% PBS-T as above, the membrane was incubated 5 minutes with approximately 400 µL luminol-peroxide solution (Clarity Western ECL Blotting Substrate, Bio-Rad) and visualized using the ChemiDoc (Bio-Rad).

Table 18: Compositions of solutions used during immunoblotting

Reagent	Components	Amounts
Transfer buffer	Milli-Q water	700 µL
	Methanol (10% V/V)	200 µL
	10x Blotting buffer (0.387 mM glycine, 0.479 mM TRIS)	100 µL
5% milk blocking solution	Milli-Q water	100 mL
	Nonfat dried milk powder	5 g
PBS-T	Milli-Q water	900 mL
	10x PBS	100 mL
	Tween 20	500 µL

Table 19: Antibody dilutions used during immunoblotting

Antibody	Dilution
α-V5 in mouse	1:2000
α-Hsp70 in mouse	1:5000
α-APRT in rabbit	1:2000
α-tubulin in mouse	1:5000
Anti-mouse	1:5000
Anti-rabbit	1:1000

3.6 IFA

The V5-tagged protein subcellular localization was analyzed by the indirect IFA technique, which uses a primary antibody specifically binding to an epitope present in the protein(s) of interest, in our case the 3xV5 epitope, encoded in the endogenous tagging products used for transfection of cells and expressed as a C-terminal translational fusion. A secondary antibody coupled to a fluorophore, in our case Alexa-488 (green) and Alexa-555 (red), then attaches to the primary antibody, allowing the visualization of the tagged protein under a fluorescent microscope through photoexcitation [47].

1 mL of culture containing *T. brucei* tagging cells were harvested at 900 g for 5 minutes at RT. After discarding the supernatant, the pellet was washed twice using Voorheis' modified PBS, vPBS, PBS supplemented with 10 mM glucose and 46 mM sucrose, pH: 7.6, and resuspended in 200 – 400 µL vPBS. 10 µL of this solution were then added to a poly-lysine coated microscope slide. After the cells decanted and adhered to the glass for 10 minutes, the upper liquid was replaced by 10 µL 4% paraformaldehyde solution and incubated for 15 minutes for fixation of the cells. Cell were permeabilized with 10 µL of 0.1% Triton-X-100 in PBS for 15 minutes. Blocking was performed with 1% BSA in PBS blocking solution with

0.033% Triton-X-100 for 1 hour. After blocking, incubation with 10 µL blocking solution containing the primary antibodies (anti-mouse α-Hsp70 as mitochondrial marker, anti-rabbit α-V5 against protein of interest), at a dilution of 1:1000 each, and was performed overnight. Then, the sample was washed thrice using PBS with 0.033% Triton-X-100 for 5 minutes each, followed by the addition of 10 µL blocking buffer containing the secondary antibodies (goat α-rabbit Alexa Fluor 488 and goat α-mouse Alexa Fluor 555 [Life Technologies]), diluted to 1:1000 each, and incubated for 1 hour. After 3 washes as above, 2 µL of ProLong 1 Gold antifade reagent containing DAPI (Molecular Probes) were added for DNA staining. The IFA was visualized using a Axioplan 2 microscope (Zeiss) coupled to a DP73 digital camera (Olympus) for picture acquisition. Images were analyzed by ImageJ [48].

3.7 Growth curves

To monitor the RNAi induced changes in growth in *T. brucei* procyclic cells, growth curves were obtained by diluting the cell cultures to a concentration of $2 \cdot 10^6$ cells/mL daily for 10 days, while adding 10 µg/mL tetracycline to the media, thereby inducing RNAi. During this process the 24-hour increase of the cell population was recorded by counting the cells with the Coulter Z2 Cell and Particle Counter (Beckman Coulter) that detects the number of cells by evaluating the electrical resistance of the sample solution, which varies depending on the number of cells present [49]. An uninduced control cell line was also subjected to this dilution scheme. To verify the successful knockdown of the tagged proteins, samples of $1 \cdot 10^7$ cells were taken each day and a WB was conducted with tubulin serving as a loading control.

4 Results

4.1 Preliminary results

Using the information available on the TrypTag database a preliminary selection of putative proteins with potential association with the TAC was conducted. Additional investigation of localization images provided by the TrypTag database and, moreover, the estimation of function and domains based on the sequences of proteins with comparable biological roles conducted to infer protein importance accompanied by literature reviews, led to further candidate prioritization and the selection of Tb13600, Tb14570, Tb840 and Tb4540 for experimental analysis to verify their presumed mitochondrial and TAC relations and examine their essentiality.

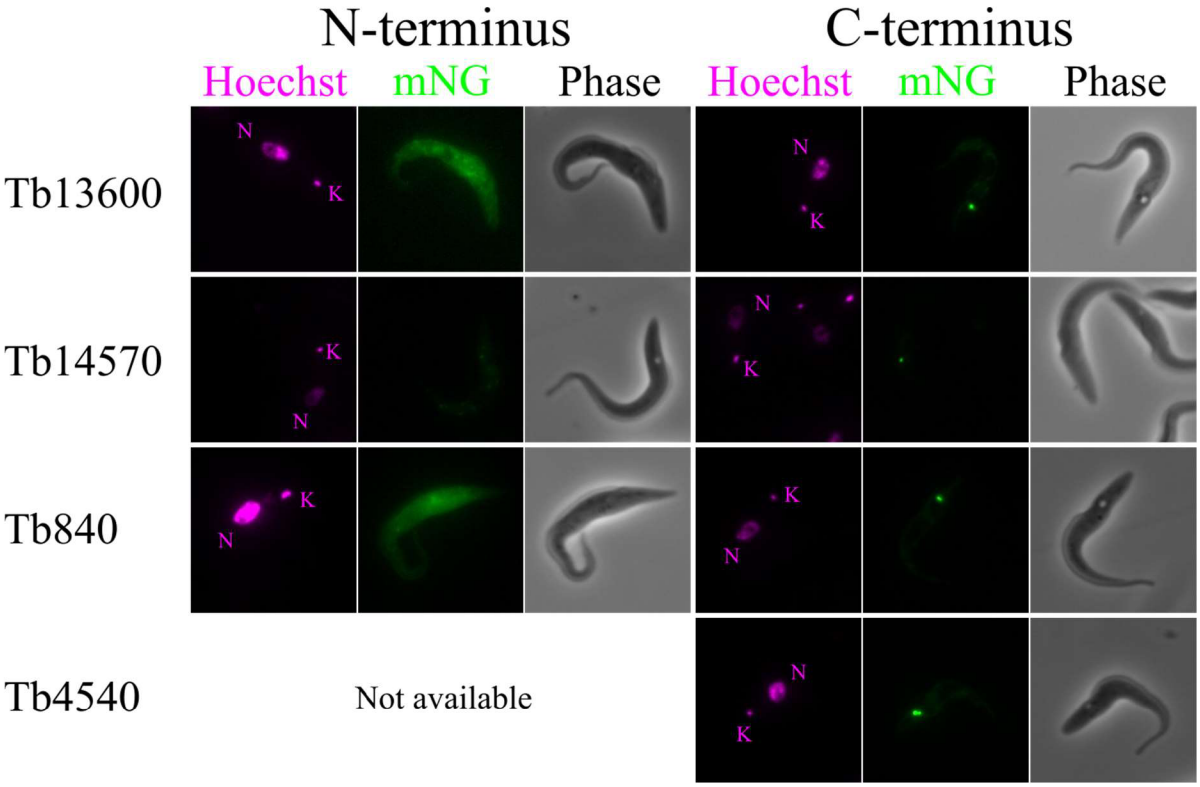

Figure 11: Localization results of N- and C-terminally tagged candidates. Hoechst staining in pink labels DNA containing structures, namely the nucleus and kinetoplast, mNeonGreen (mNG) in green labels the subcellular distribution of either N- or C-terminally tagged proteins, denoted by the acronym on the left side. The kinetoplast and nucleus are additionally indicated by a pink K and N next to them in the images showing the Hoechst-stained cells. In all cases, C-terminal tagging results indicated a TAC relation evidenced as a punctual distribution close to the kinetoplast.

The mNeonGreen tagging images provided by the TrypTag database and shown in Figure 11 show cytoplasmic localization of all N-terminally tagged candidates that could be caused by the presence of a possible translocation signal inferred by expression of mNeonGreen. C-terminally tagged proteins displayed a clear relation to the TAC in addition to an association

to the mitochondrion itself or the kinetoplast DNA. This led to the decision to tag the proteins with the 3xV5 epitope at the C-termini to validate this observed localization.

4.2 Bioinformatic analysis and curation of prioritized proteins

In this section the putative inferred domains and main features for the prioritized proteins examined in this thesis will be shortly listed.

4.2.1 DnaJ domain containing protein, putative (Tb13600)

Tb13600 is a putative DnaJ domain containing protein. Proteins with J-domains in *T. brucei* serve as chaperones in protein assembly, are engaged in protein transport, avert accumulation of misfolded proteins and are known co-chaperones to Hsp70[50,51]. These types of polypeptides have been previously localized in both the mitochondrion and cytoplasm [50].

4.2.2 LicD family, putative (Tb14570)

Tb15470 is a proposed LicD enzyme. These types of proteins are known for their role in the bacterial phosphocholine metabolism, during which they attach phosphocholine to the glycans, exhibiting transferase activity [52]. Tagging of LicD enzymes in *Streptococcus pneumoniae* revealed their localization in the cell membrane, where they attach choline to teichoic acid found in the cell wall [53]. Another postulated function is their involvement in the transport of various types of sugars as catalysts [54].

4.2.3 Histidine kinase-, DNA gyrase B-, and HSP90-like ATPase, putative (Tb840)

Tb840 bears an inferred ATP binding domain found in histidine kinases, DNA gyrases and Hsp90 chaperones. These proteins, which share the need for ATP to fuel their metabolic functions, are involved in biological processes like histidine phosphorylation, DNA repair and replication, as well as protein folding [55].

4.2.4 3-hydroxy-3-methylglutaryl-CoA reductase, putative (3-HMG-CoA reductase, Tb4540)

Tb4540 is a putative 3-HMG-CoA reductase. This protein takes part in isoprenoid biosynthesis by producing mevalonate through reduction of 3-HMG-CoA and was already detected in *T. brucei* mitochondria [56,57]. Pharmacological inhibition of 3-HMG-CoA activity led to growth defects of *T. brucei* in both procyclic and bloodstream cells [58].

4.3 Subcellular localization analysis by endogenous V5 tagging

4.3.1 PCR generation of tagging constructs

To generate the amplicons for the 3xV5 epitope *in-situ* C-terminal tagging of the proteins examined and subsequent localization using anti V5 specific antibodies, long primer PCR using a pPOTv4 [25] modified vector termed pPOTv5 (Figure 12) as template was performed, leading to the generation of the tagging cassette (Figure 13). Primers for these amplicons attach to the template plasmid along a length of 18 and 20 bps for the forward and reverse primer respectively and amplify a sequence containing the 3xV5 tag and a hygromycin resistance gene. After PCR, amplicons were inspected to verify the generation of the tagging construct by running 5 µL of the PCR reaction in 1% agarose gels (Figure 14). Each PCR product had a length of approximately 2000 bps. Thereafter, transfection of procyclic *T. brucei* and subsequent selection using hygromycin was performed as detailed above.

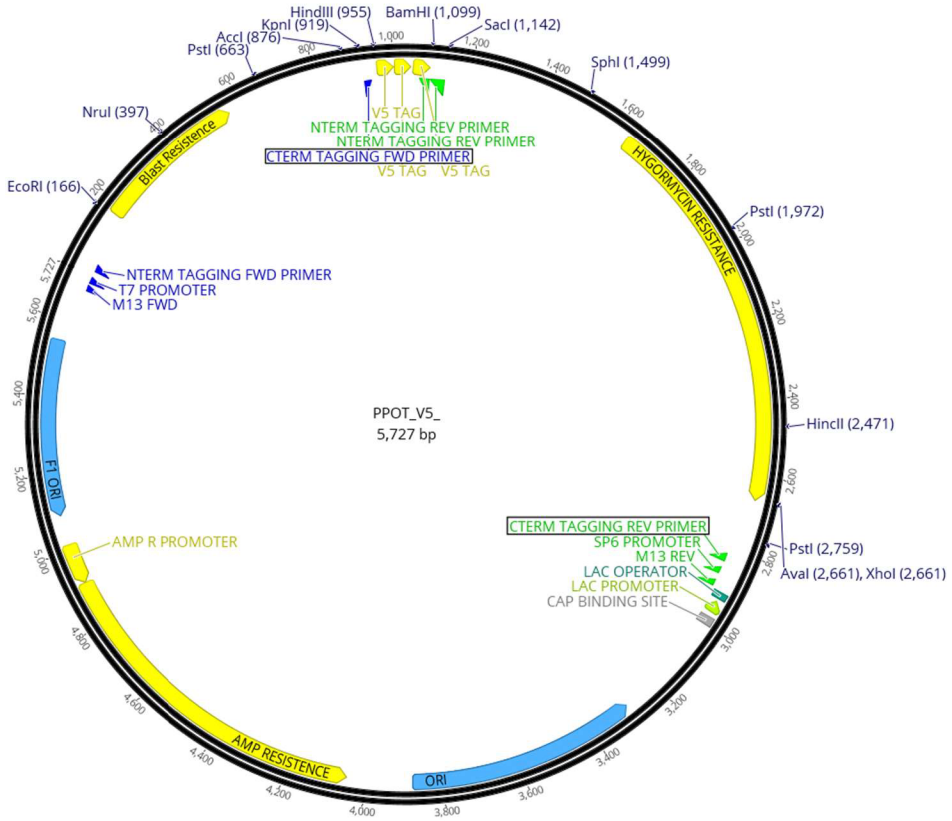

Figure 12: Scheme of the pPOTv5 vector. Yellow regions indicate antibiotic resistance genes, the light blue regions origins of replications (ORI) of the plasmid. Restriction sites are denoted in dark blue colored and include their position in brackets. The primers and their attachment sites used for C-terminal tagging are highlighted by black boxes. The 3xV5 tag is situated on top of the plasmid and depicted by 3 small yellow arrows.

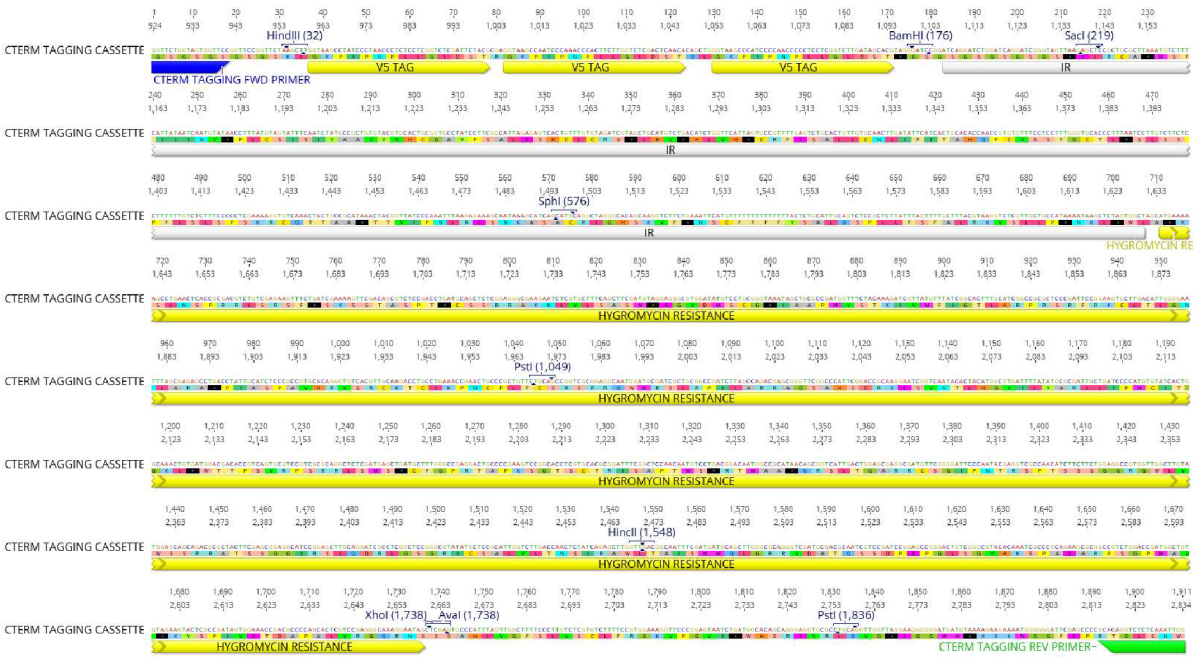

Figure 13: Scheme of C-terminal tagging cassette generated through PCR using the pPOTv5 template. The blue arrow indicates the CTERM TAGGING FWD forward primer while the CTERM TAGGING REV reverse primer is highlighted in green. Restriction sites are denoted in dark blue and include their position in brackets. In the first row the 3xV5 epitope is indicated by three yellow arrows. IR, here the grey arrow, stands for intergenic region, necessary for the transcription of the tagged ORF and the hygromycin resistance gene, also indicated by a yellow arrow.

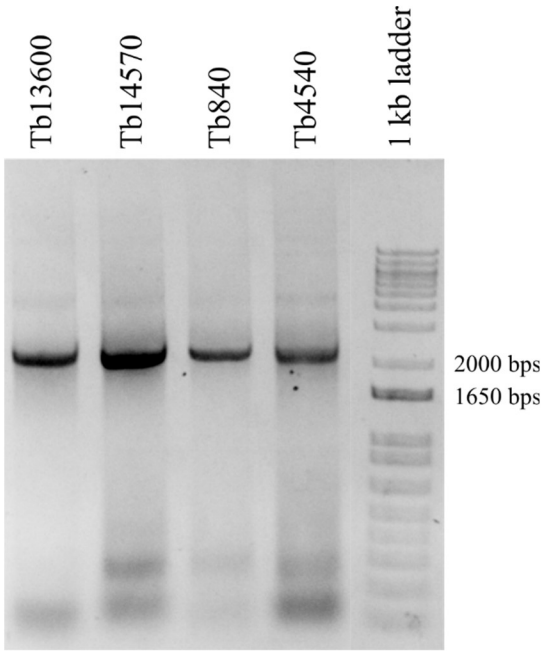

Figure 14: Verification of the amplicons for endogenous tagging using long primers and pPOTv5 as template. The acronyms stand for the PCR products of the respective targeted genes. The length of the strands of the 1 kb ladder are indicated in bp and enable the identification and measurement of the amplicons based on size.

4.3.2 Indirect IFA validation of the subcellular localization of prioritized proteins

To validate the subcellular localization reported in TrypTag, IFA was conducted on the V5 tagged cell lines using an anti V5-specific antibody to localize the tagged proteins within the cells. Antibodies against the mitochondrial protein Hsp70 were applied as markers of this organelle and DAPI as for staining the DNA situated in the nucleus and kinetoplast.

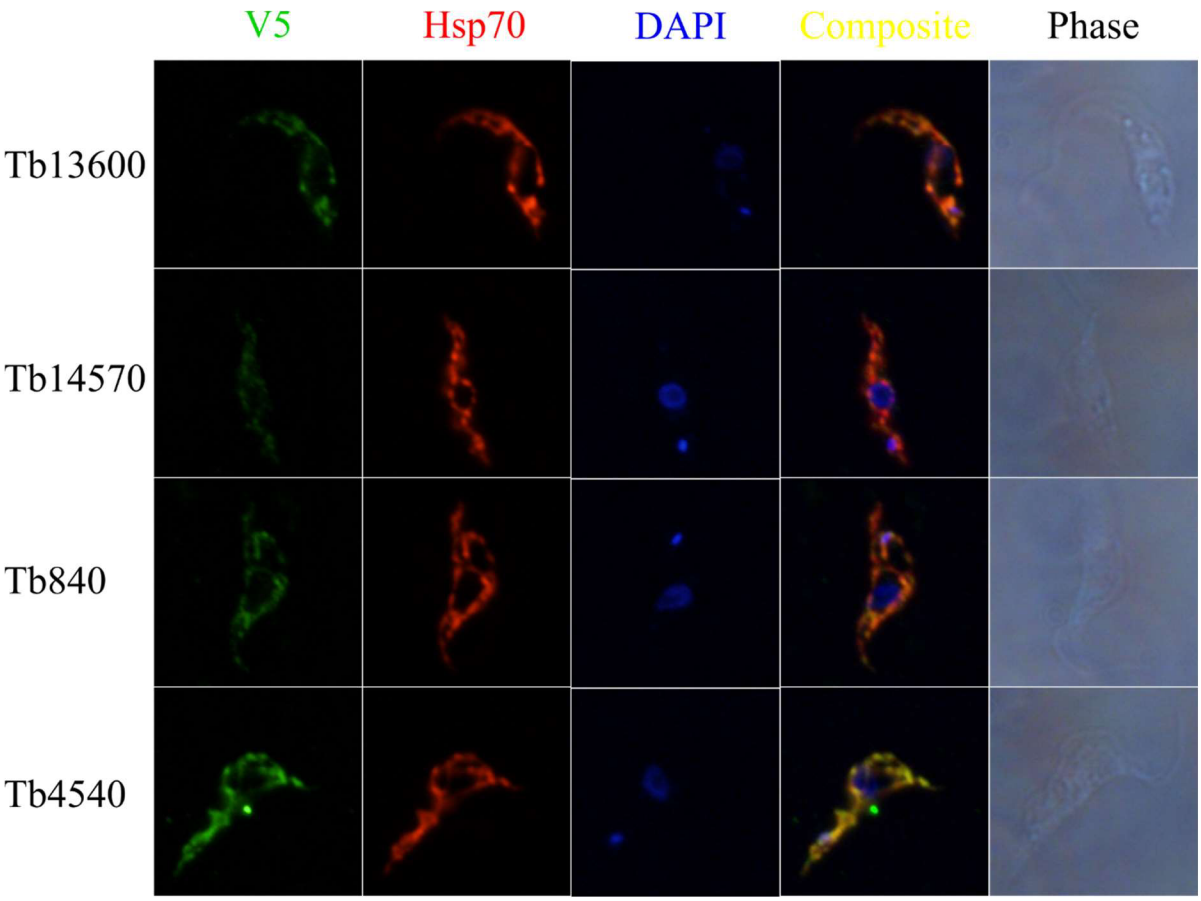

Figure 15: Pictures showing the fluorescent 3xV5 tagged protein in green, the mitochondrial marker Hsp70 in red and DAPI stained nuclear and kinetoplast DNA in blue. The composites are a merged picture of the colorized images, the phase shows the cell body. The acronyms on the left side indicate the respective C-terminally tagged proteins that are investigated.

As shown in Figure 15, Tb13600, Tb14570, Tb840 and Tb4540 the 3xV5 signal colocalized in all cases with the Hsp70 signal, indicating a mitochondrial localization for the proteins of interest. Also, no evident enrichment in the region close to the kinetoplast was observed. This contrasted with the reported "TAC-related" localization reported in TrypTag.

4.3.3 Subcellular localization WB analysis of crude digitonin fractionation

As an alternative approach to IFA for validation of subcellular localization, further analysis was conducted *via* crude subcellular fractionation with digitonin followed by WB. This procedure was performed to fractionate proteins in the whole cell lysate into a cytoplasmic and a mitochondrial fraction through digitonin directed differential cell lysis, enabling the subsequent allocation of the tagged proteins, as detailed in the methods section. V5, Hsp70 and APRT specific antibodies were used for the detection of the tagged proteins, the mitochondrial and the cytoplasmic fraction respectively. APRT constitutes as a marker for the cytoplasmic fraction due to its consistent expression in all *T. brucei* cell types and previous

use as a cytoplasmic control in both IFA and WB experiments, which is also the case for the mitochondrial marker Hsp70 [59].

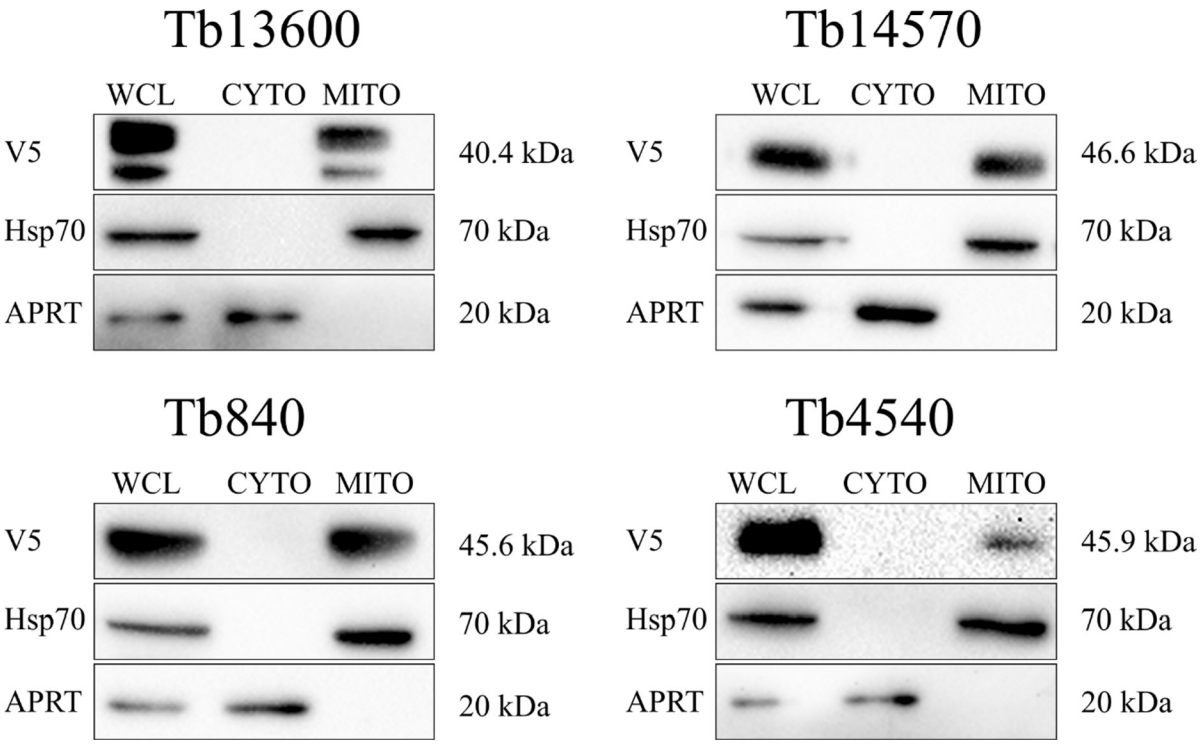

Figure 16: WB results of digitonin crude cellular fractionation with the acronyms corresponding to the respective examined proteins. The whole cell lysate (WCL), cytoplasmic (CYTO) and mitochondrial (MITO) fractions were subjected to immunoblotting with anti V5 specific antibodies to enable the localization to either the CYTO or MITO fraction of the selected proteins. Antibodies against Hsp70 and APRT served as controls for the MITO and CYTO fractions respectively. Protein molecular weights are indicated in kDa for both controls and proteins.

The WBs shown in Figure 16 localized Tb13600, Tb14570, Tb840 and Tb4540 in the mitochondrial fraction, consistent with the results obtained by the IFA analysis. Decreased band intensities of the WCL compared to the mitochondrial fractions indicate that during the digitonin fractionation the mitochondrial sample was diluted. The higher concentration of the WCL then results in a band with increased intensity compared to the MITO fraction.

The protein weights of Tb13600, Tb14570, Tb840 and Tb4540 were calculated from the sequences extracted from the TriTrypDB using the molecular weight calculator tool provided by www.web.expasy.org, obtaining the following numbers: Tb13600 weighing 40.4 kDa, Tb14570 46.6 kDa, Tb840 45.6 kDa and Tb4540 45.9 kDa. These molecular weights are in accordance with protein sizes detected experimentally with WB [60].

4.4 RNAi knockdown of the selected proteins

4.4.1 Amplification of the RNAi targeted gene sequence

To generate the gene insert enabling RNAi of the proteins of interest PCR was conducted over *T. brucei* TREU 927/4 gDNA. Correct amplification of the sequence was verified through agarose gel electrophoresis, shown in Figure 17.

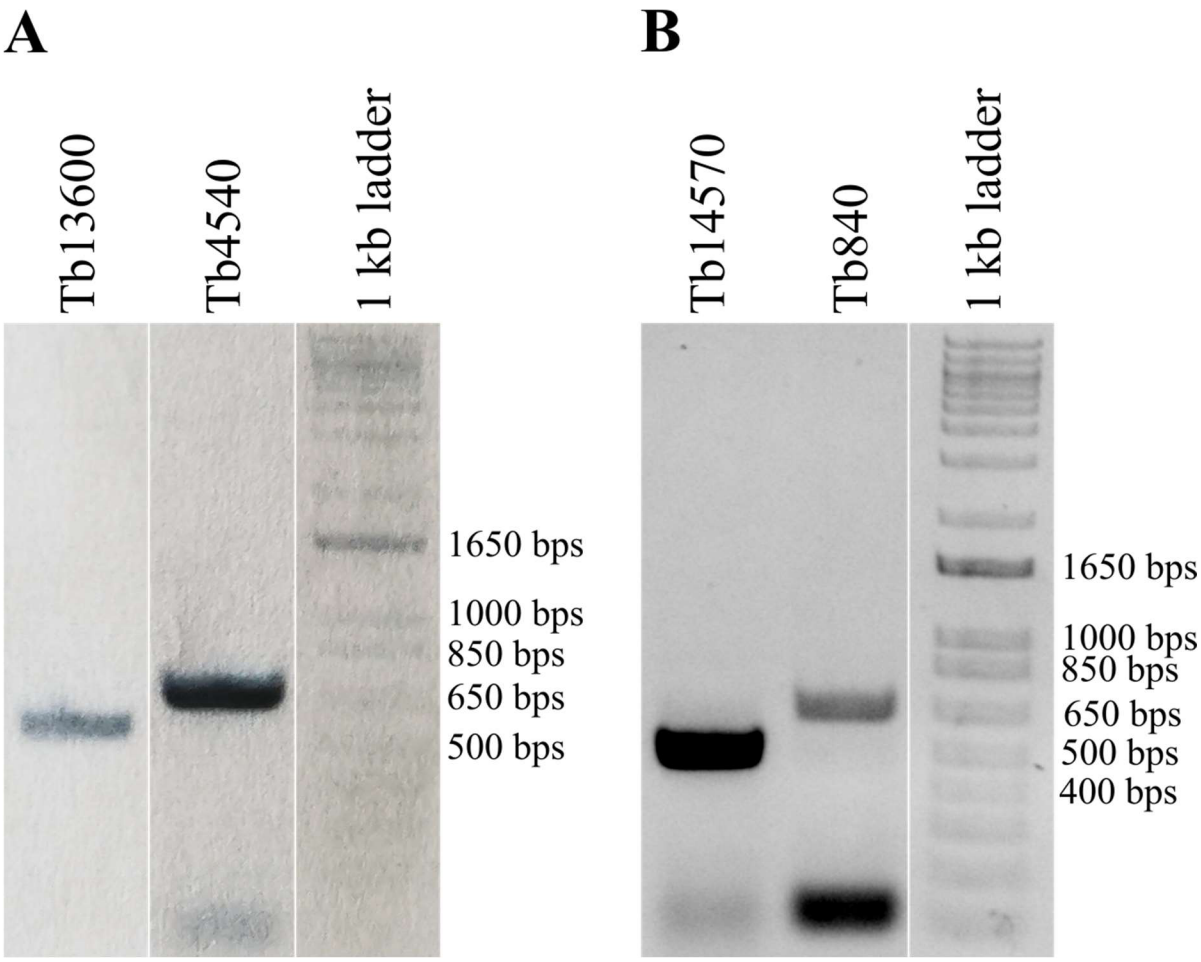

Figure 17: Agarose gel electrophoreses after PCR over gDNA for amplification of Tb13600, Tb14570, Tb840 and Tb4540 (acronyms) RNAi targeted genetic sequences. The length of the strands of the 1 kb ladder are indicated in bp and enabled the identification and measurement of the amplicons based on size. All amplicons have the expected sizes that varied between 500 and 650 bps. Panels A and B represent two independent PCR amplification reactions, both generating the desired products.

Figure 17 A depicts the results of the PCR reactions which demonstrate the amplification of the Tb13600 and Tb4540 sequence. Due to the failed generation of the Tb14570 and Tb840 PCR products, the experiment was repeated for these proteins with no changes to the procedure, visible in Figure 17 B.

The agarose gel electrophoreses confirmed the expected length of all obtained amplicons. Subsequently, the PCR products were purified and utilized in Gibson assembly reactions in combination with stuffer, plasmid backbone and 2x Gibson assembly master mix solutions to

produce the respective pTrypSon vectors. Then, transformations of the assembly reactions into competent *E. coli* through heat shock and plating onto agar plates were conducted to isolate positive clones validated by colony PCR, restriction digests and sequencing.

4.4.2 Colony PCR screening

Colony PCR screenings of selected clones from the transformed *E. coli* plates were performed to infer if the plasmid was correctly assembled from its constituents, namely the gene specific inserts, the stuffer and the plasmid backbone. The PCR reaction was performed using the respective RNAi forward primers and a gRNAi SEQ reverse primer and led to the generation of amplicons that include the gene insert and a part of the stuffer. Their binding sites are indicated in the Figures 18 and 19, depicting generalizations of the RNAi colony PCR cassette and the assembled pTrypson plasmid, respectively.

Figure 18: Scheme of a generalized RNAi colony PCR sample cassette of a centrin containing pTrypson vector (modified from [27]) Primer binding sites are highlighted by blue or green arrows. The primers used during colony PCR are highlighted by black boxes. Additionally, restriction sites, most importantly XhoI and HindIII, are denoted in dark blue with their position in brackets.

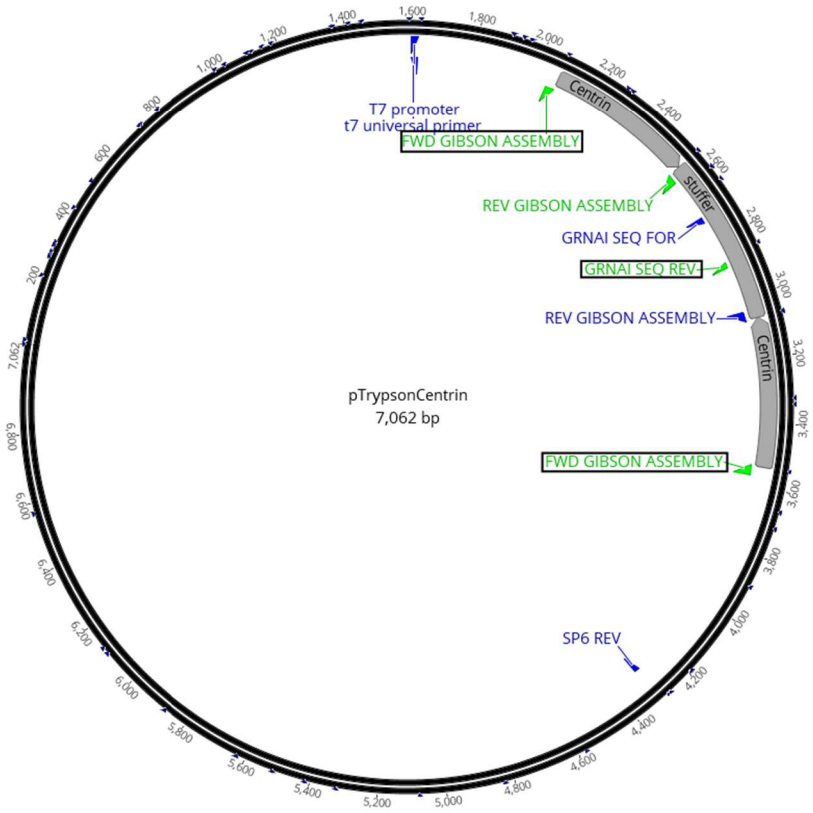

Figure 19: Scheme depicting a generalization of a correctly assembled pTrypson vector. Here, the gene insert codes for a centrin gene (modified from [27]). In this thesis sequences coding for the genes of interest are used instead. The stuffer and gene insert sequences are depicted by grey arrows. The primers used to infer the correct plasmid assembly are highlighted by black boxes. Each primer, in either blue or green, is depicted at their respective binding sites.

Figure 20 shows the agarose gel of the first round of colony PCRs conducted. The bands found in the lanes for the colonies 1 and 13 suggested the successful transformation of the Tb13600 and Tb840 vector into *E. coli*. A restriction check through digestion of the plasmids found in 1 and 13 and, additionally, in the colonies 13, 16 and 24 using XhoI and HindIII-Hf depicted in Figure 21 confirmed the assumption. The signal at 5000 bps is the plasmid backbone while the faint bands found between 500 and 650 bps are the genes of interest.

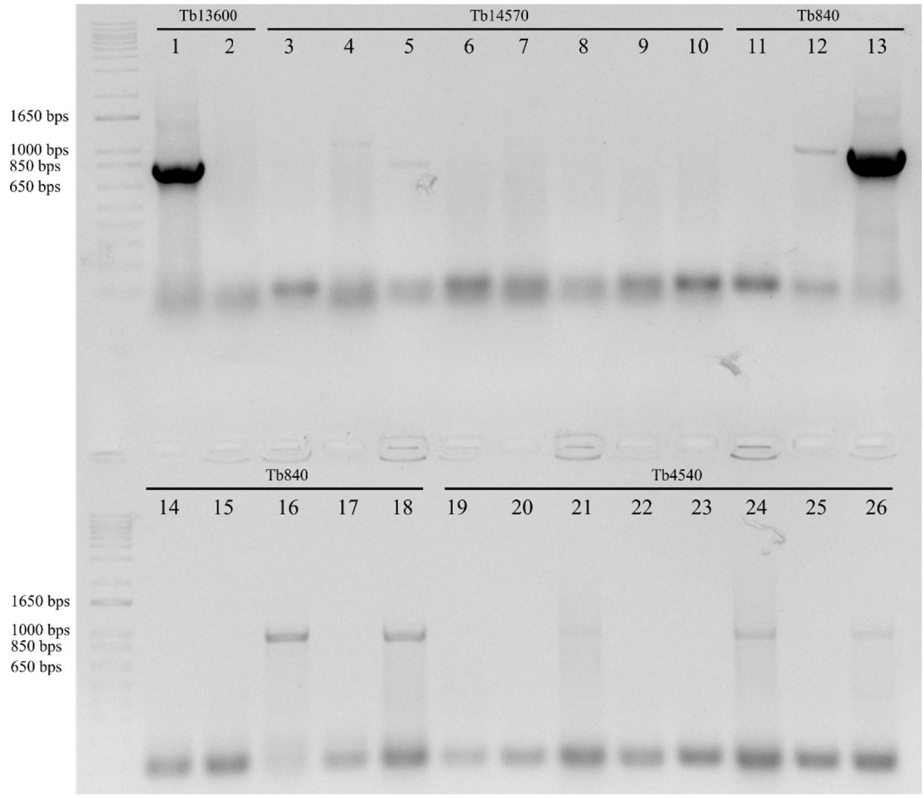

Figure 20: Agarose gel electrophoresis depicting the results of the first colony PCR. 1-2 were Tb13600 colonies, 3-10 Tb14750, 11-18 Tb840 and 19-26 Tb4540. The length of the strands of the marker used (1 kb ladder) are indicated in bp and enable the identification and measurement of the amplicons based on size. The expected size of obtained products range between 650 and 850 bps.

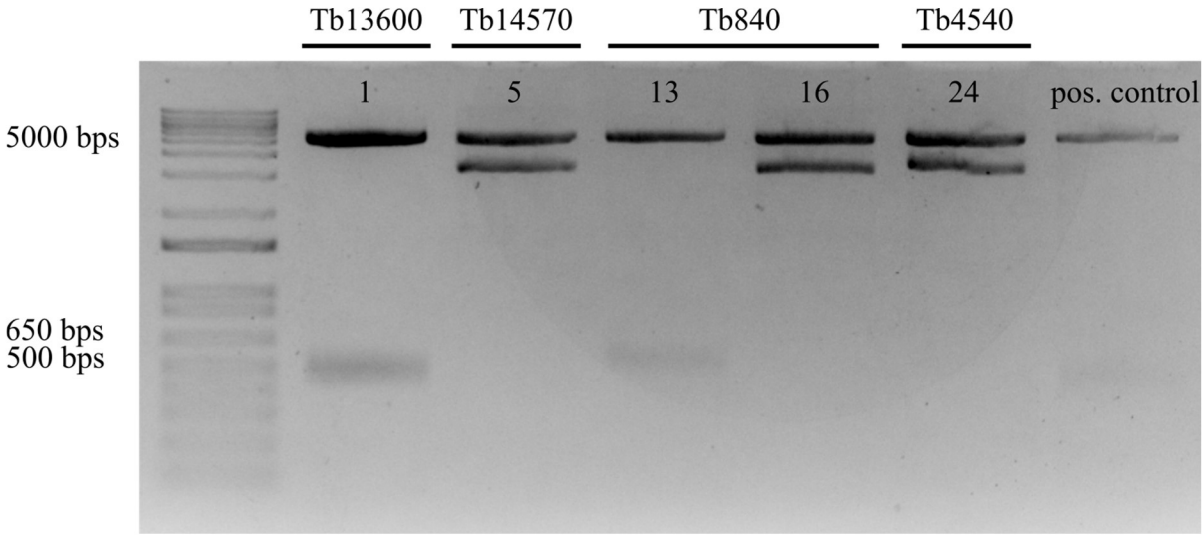

Figure 21: Restriction check by digestion with XhoI and HindIII-Hf for colonies 1, 5, 13, 16 and 24. A pTrypson plasmid served as positive control. The expected sizes from the gene inserts between 500 and 650 bps coincide with the sizes from the generation of the RNAi amplicons.

A second colony PCR using colonies transformed with plasmids containing the inserts of Tb14750 and Tb4540 was performed and resulted in a positive signal for colony 50 visible in Figure 22. The digestion of the Tb4540 plasmid during the restriction check, depicted in Figure 23, reinforced this assumption, resulting in distinct backbone and insert signals at around 5000 bps and between 400 and 500 bps respectively.

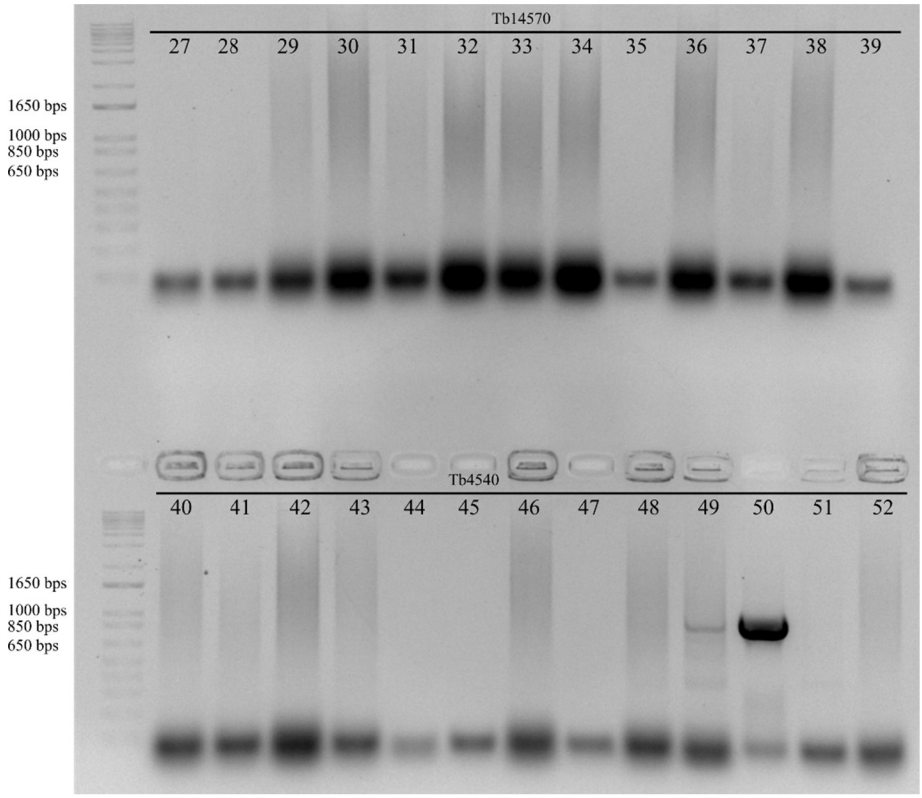

Figure 22: Agarose gel electrophoresis depicting the results of the second colony PCR. Colonies 27-39 were Tb14750, 40-52 Tb4540. The length of the strands of the marker used (1 kb ladder) are indicated in bp and enable the identification and measurement of the amplicons based on size. The expected size of the obtained product ranges between 650 and 850 bps.

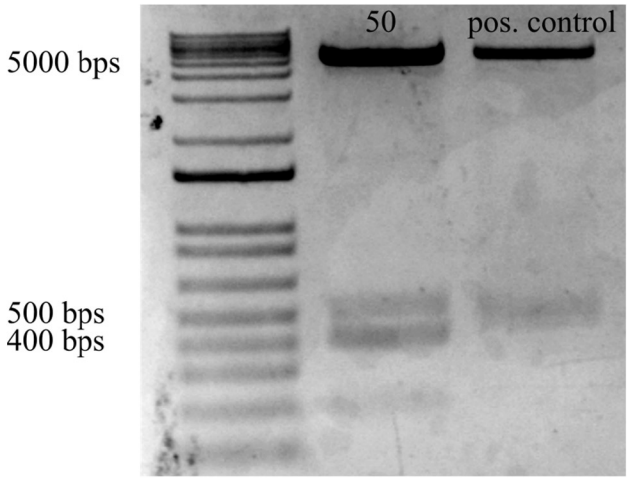

Figure 23: Restriction check by digestion with XhoI and HindIII-Hf for colony 50. A pTrypson plasmid served as positive control. The expected size from the gene insert at approximately 500 bps coincides with the size from the generation of the RNAi amplicons.

From the third colony PCR performed solely with Tb14750 colonies and only one positive product from the 66th screened colony was retrieved. A restriction check confirmed the positivity and led to the backbone signal at around 5000 bps and the gene insert band between 500 bps and 650 bps.

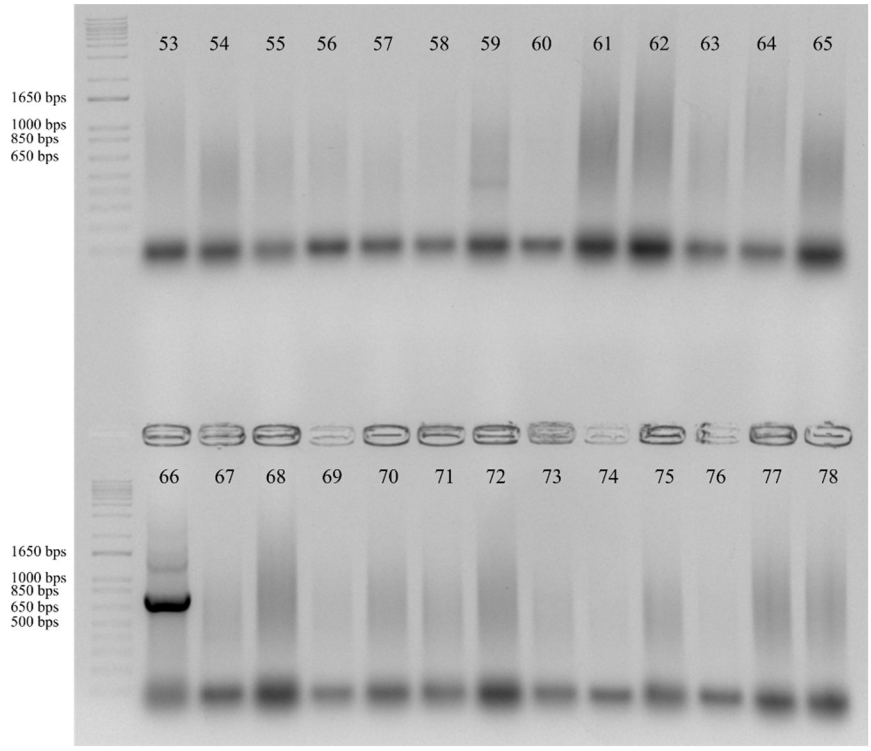

Figure 24: Agarose gel electrophoresis depicting the results of the third colony PCR. All colonies (53-78) contained Tb14750 plasmids. The length of the strands of the marker used (1 kb ladder) are indicated in bp and enable the identification and measurement of the amplicons based on size. The expected size of the obtained product is 650 bps.

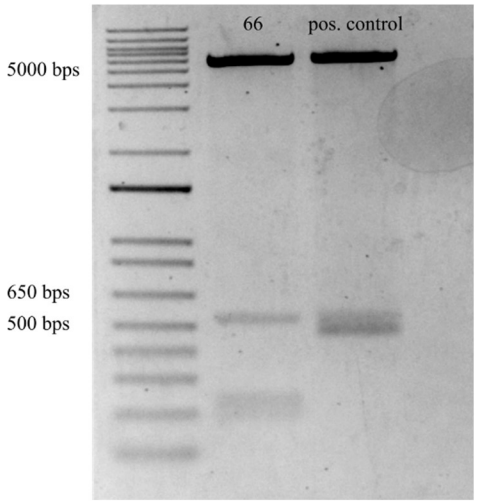

Figure 25: Restriction check by digestion with XhoI and HindIII-Hf for colony 66. A pTrypson plasmid served as positive control. The expected size from the gene insert lies between 500 and 650 bps and coincides with the size from the generation of the RNAi amplicons.

Following colony PCRs and restriction checks plasmid samples of all positive colonies were sent to sequencing for verification of their sequence. Figure 26 depicts an example, in our case Tb13600, for a consensus obtained from the sequencing results obtained by sequencing with primers gRNAi SEQ forward and reverse.

Figure 26: Scheme as an example of a consensus sequence obtained from sequencing results. Primer binding sites for gRNAi SEQ forward and reverse are in blue and green. The stuffer is depicted by a grey arrow, the two inverted repeats of the sequence inducing RNAi (here for Tb13600) are highlighted by white and yellow arrows. Restriction sites XhoI and HindIII are denoted in grey with their position in brackets. Additionally, the BLAST result of the targeted RNAi fragment is also shown.

After the confirmation of the DNA sequences needed for RNAi, the number of transformed bacteria from positive colonies was augmented in LB media with ampicillin and the plasmids extracted with the Miniprep kit. Subsequent linearization of the vectors with NotI-Hf was conducted to enable correct recombination for transfection procedure that followed.

4.4.3 Growth curve

To assess the viability in terms of growth of the cells after RNAi knockdown, and therefore the essentiality of the selected targets, standard growth curves were performed. The growth of transfected RNAi cell lines after tetracycline induced RNAi expression was monitored for 10 days and compared to an uninduced cell line. Both the uninduced control and the induced cells were counted and diluted daily to a concentration of $2 \cdot 10^6$ cells/mL. The graphics correspond to the cumulative cell growth. To evaluate RNAi mediated knockdown of protein expression, WB was performed afterwards with samples from day 0 to 8 consisting of $1 \cdot 10^7$ cells.

As seen in Figure 27, the RNAi induced knockdown of Tb13600 protein expression led to a minor decrease in cell division compared to the uninduced control cell line. In agreement with this, Figure 28 shows that after 8 days of tetracycline addition the protein was still expressed

to significant levels, indicating that RNAi knockdown did not fully ablate the protein levels, and therefore, could explain the absence of a clear growth phenotype.

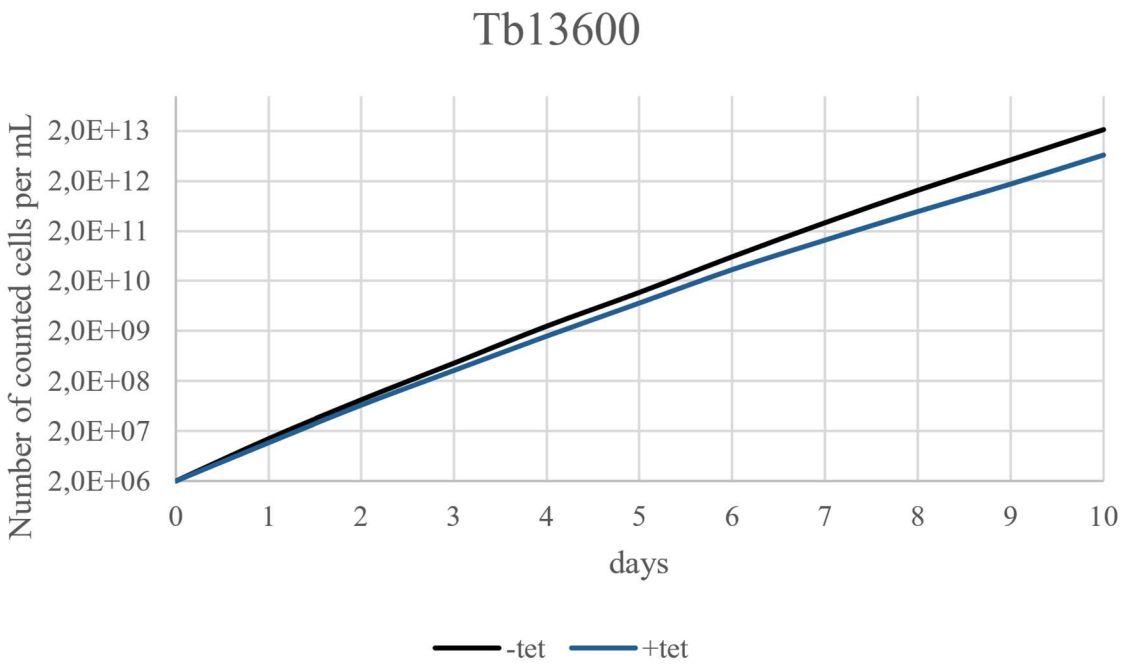

Figure 27: Logarithmic growth curve diagram for Tb13600; -tet indicates the uninduced cell line in black, +tet the induced cell line in blue.

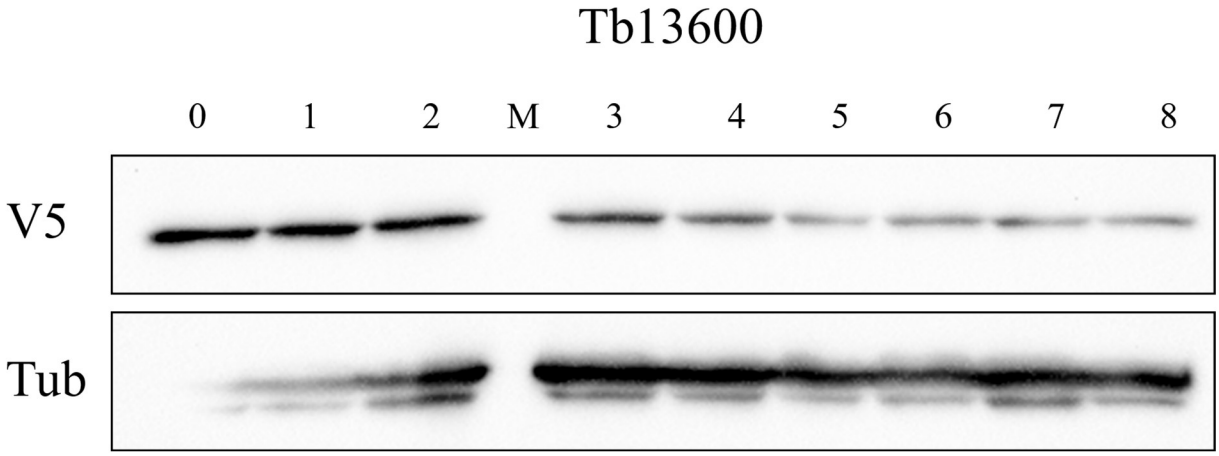

Figure 28: WB of samples of Tb13600 taken each day during the growth curve measurements from the induced cell line. The numbers (0-8) indicate the days post induction. V5 expression was examined while tubulin (Tub) served as loading control. M indicates the marker.

The RNAi of Tb14570 did not have any significant influence on the growth of *T. brucei* according to Figure 29. Subsequent WB investigation indicates that the RNAi itself led to undetectable levels of protein expression, as it is shown in Figure 30.

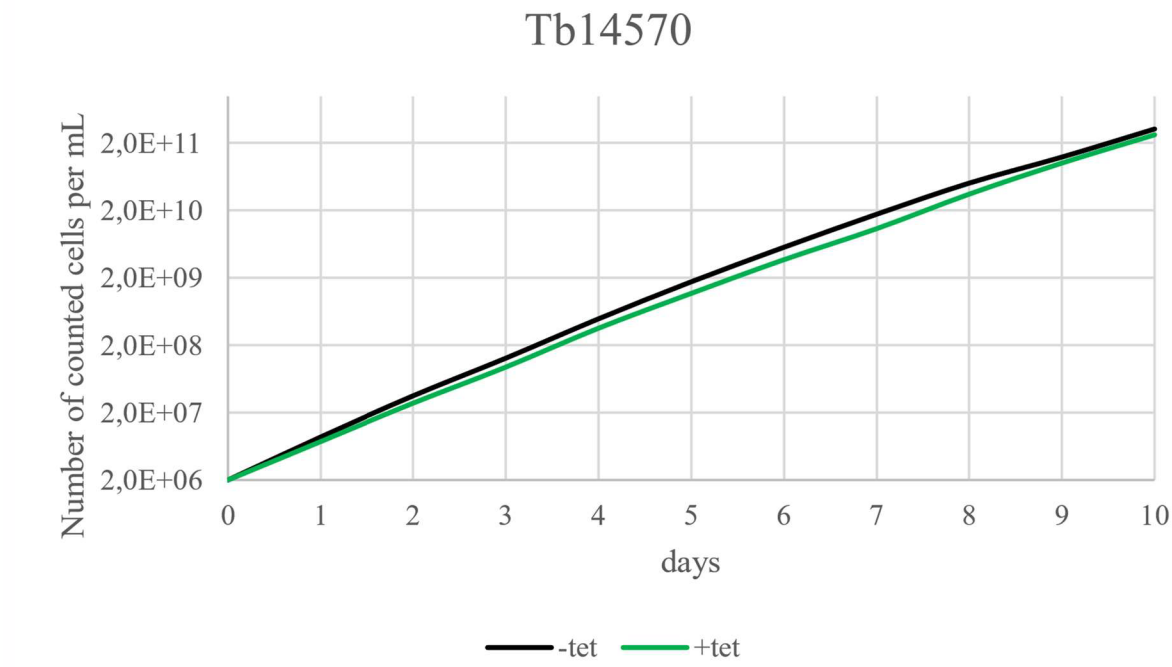

Figure 29: Logarithmic growth curve diagram for Tb14570; -tet indicates the uninduced cell line in black, +tet the induced cell line in green.

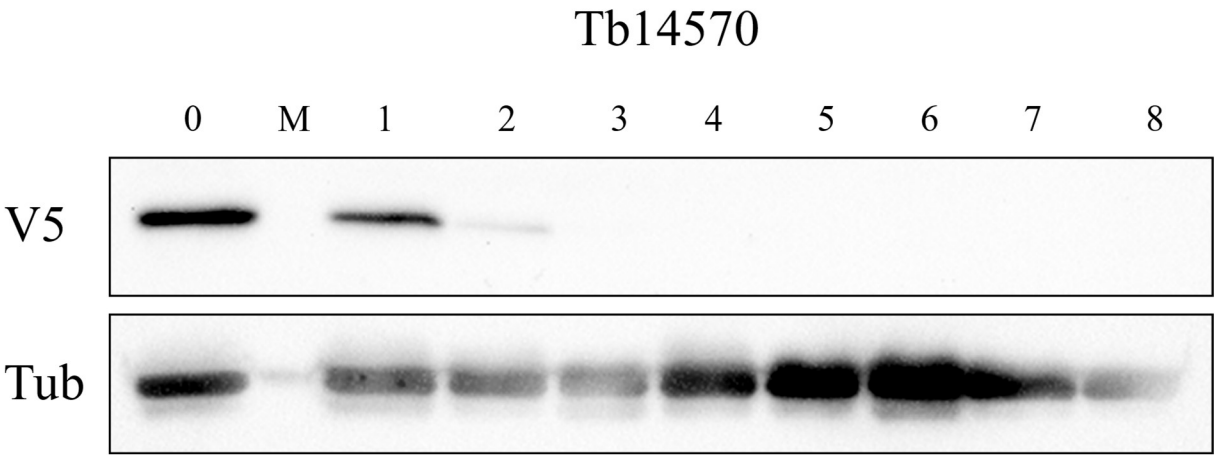

Figure 30: WB of samples of Tb14750 taken each day during the growth curve measurements from the induced cell line. The numbers (0-8) indicate the days post induction. V5 expression was examined while tubulin (Tub) served as loading control. M indicates the marker.

The growth phenotype of the Tb840 cell line with induced RNAi compared to the uninduced control indicates a mildly decreased cell division frequency, seen in Figure 31. Figure 32 shows an inconclusive WB, which may have been caused by insufficient ECL application or incomplete protein transference. This experiment was not repeated.

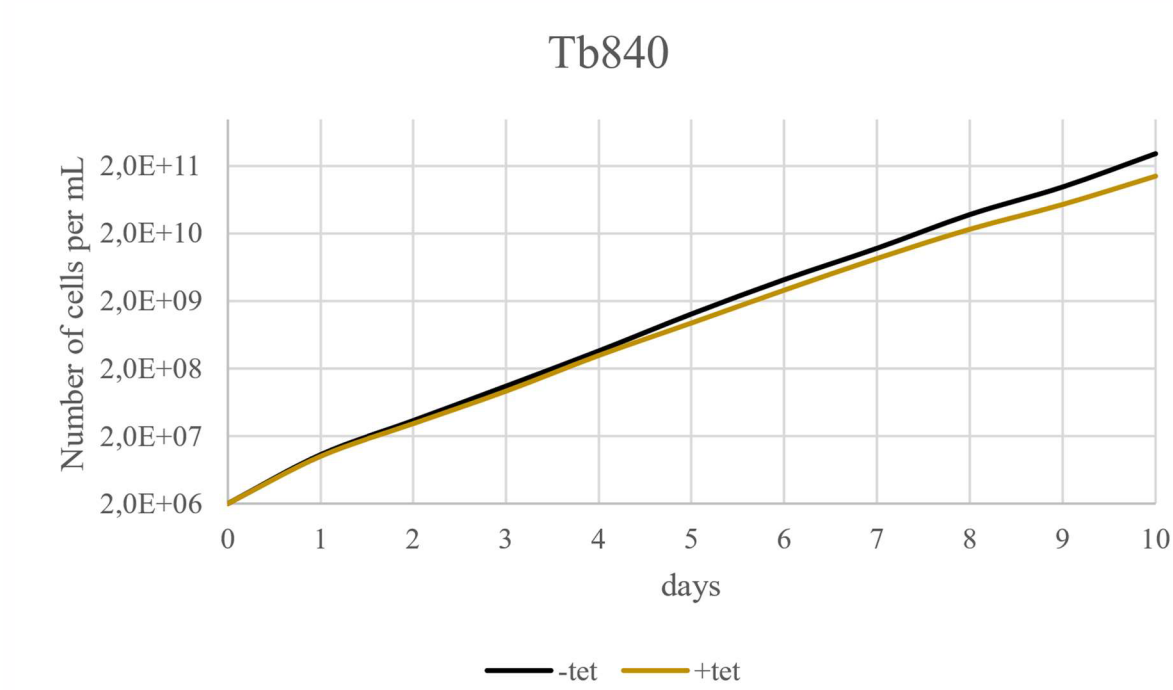

Figure 31: Logarithmic growth curve diagram for Tb840; -tet indicates the uninduced cell line in black, +tet the induced cell line in yellow.

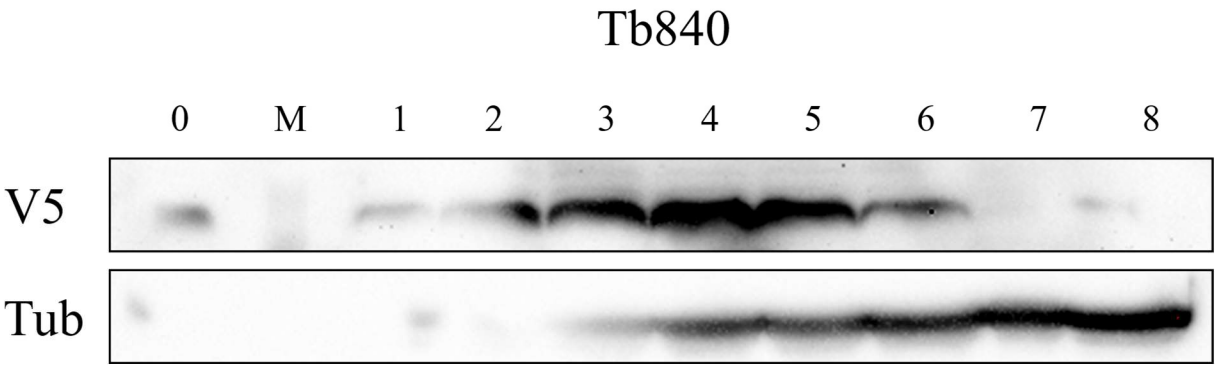

Figure 32: WB of samples of Tb840 taken each day during the growth curve measurements from the induced cell line. The numbers (0-8) indicate the days post induction. V5 expression was examined while tubulin (Tub) served as loading control. M indicates the marker.

Figure 33 shows a growth phenotype with a significant decrease in the induced Tb4540 cell line and a complete stop of cell division from day 6 onward, preventing the taking of a WB sample with $1 \cdot 10^7$ cells. Consequently, the WB only contains samples from day 0 to 6 of tetracycline induction. Furthermore, the WB indicates the complete suppression of protein expression after day 4 of tetracycline addition.

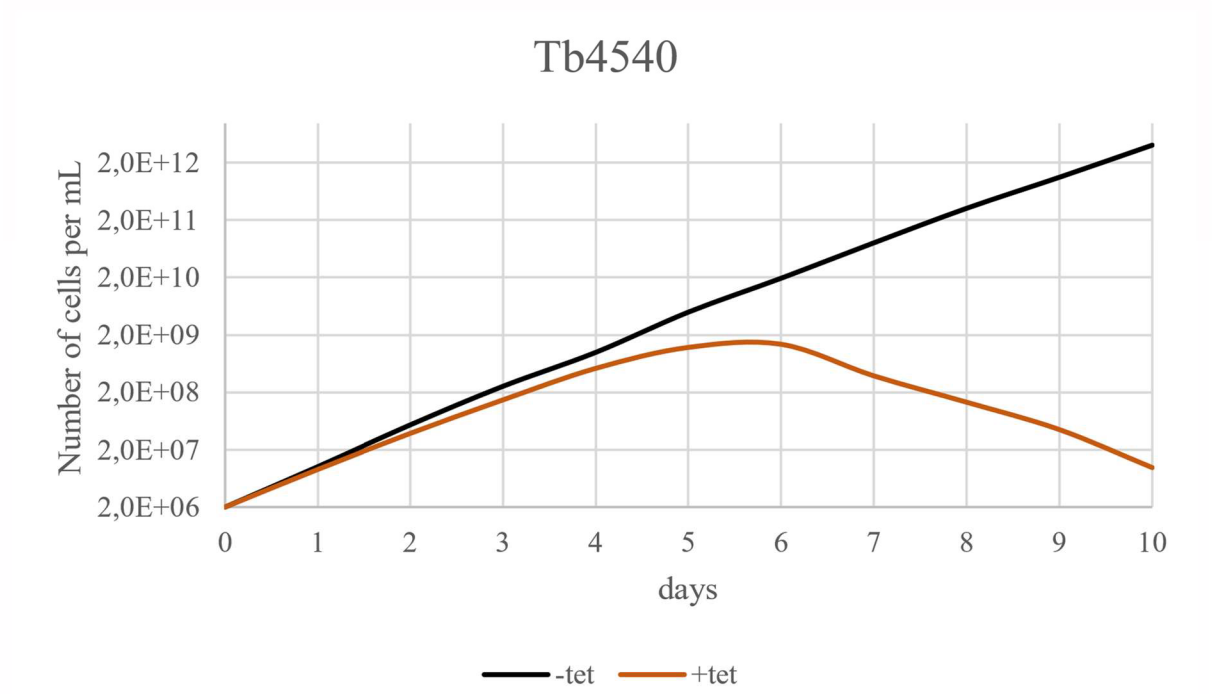

Figure 33: Logarithmic growth curve diagram for Tb4540; -tet indicates the uninduced cell line in black, +tet the induced cell line in brown.

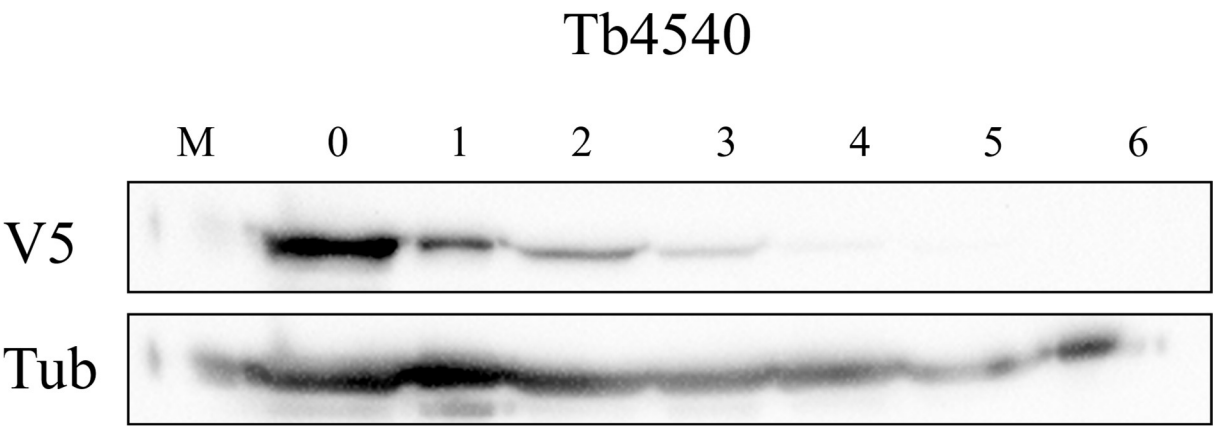

Figure 34: WB of samples of Tb4540 taken each day during the growth curve measurements from the induced cell line. The numbers (0-6) indicate the days post induction. V5 expression was examined while tubulin (Tub) served as loading control. M indicates the marker.

5 Discussion

5.1 Subcellular localization analysis

According to the annotations acquired from the TrypTag database the proteins Tb13600, Tb14570, Tb840 and Tb4540 are presumably localized in the mitochondrion and may exhibit an additional relation to the TAC or the kinetoplast DNA. Experimental localization was carried out through tagging the candidates at the C-terminus with the 3xV5 epitope and performing an IFA with the mitochondrial marker Hsp70 to verify the information provided by TrypTag. The signals of all four tagged proteins of interest colocalized with their respective Hsp70 signals, indicating a relation to the mitochondrion. However, in contrast to the TrypTag annotations, no connection to the TAC or the kinetoplast DNA was indicated during this experiment. Additionally, WBs of crude cellular fractionation samples were conducted with Hsp70 and APRT as markers for the mitochondrial and cytoplasmic fractions for additional validation of the localizations obtained from the IFAs. The proteins were detected in the whole cell lysate and mitochondrial fractions, again indicating a localization within the mitochondrion, in total agreement with the previous detections. These findings also match with a mitochondrial proteomic analysis of procyclic cells *via* mass spectrometry conducted by Panigrahi et al., which detected all herein studied proteins in the *T. brucei* mitochondrion [21]. Additionally, localization of Tb4540 to the mitochondrial matrix was already experimentally verified [56,61]. Thus, our results suggest that the "TAC-related" localization from TrypTag project is artifactual.

For Tb14570, a putative LicD family protein, the TAC annotation was considered relevant due to the postulated relation to the mitochondrial membrane that proteins with related homology inferred domains exhibited in interactions with lipid domains [53]. However, our results again rather point out that this localization most probably is due to an artifact derived from mNeonGreen expression, as it seemed to be the case for all proteins studied here.

5.2 RNAi and growth curve

By performing a tetracycline induced RNAi knockdown of the proteins of interest their essentiality was examined by measuring the cell growth of single clone cell lines after induction of RNAi for 10 days. A previous high throughput RNAi screening performing RNAi on more than 90000 *T. brucei* proteins, including the candidates of this thesis, reported a significant growth phenotype for Tb13600 in a bloodstream form cell line only, which was not

evaluated in the present study, while Tb14570, Tb840 and Tb4540 expressed no change in growth behavior in all examined developmental stages, namely bloodstream cells after three and six days of tetracycline addition, as well as procyclics and intermediary stage cells [62]. These findings are in accordance with our results for Tb14570, which exhibited no significant growth defect after a complete protein knockdown, possibly caused by a functional redundancy of the protein.

In the Tb13600 cell line RNAi led to a mild decrease in growth and a decreased but still detectable level of protein expression. The remaining Tb13600 protein may account for the lack of a growth phenotype. Therefore, both increasing tetracycline levels and targeting a different region within the coding sequence for RNAi might bring different results. Nevertheless, this was not conducted.

The knockdown of Tb840 resulted in a decrease in cell division. However, the subsequent WB results were inconclusive due to technical errors, preventing the examination of the protein levels of the relevant growth curve samples.

Results from the RNAi of Tb4540 suggest a termination of cell division accompanied by a complete prevention of protein expression from days 6 and 4 of tetracycline expression onward respectively. These findings mimic the pharmacologically growth phenotype in both procyclic and bloodstream *T. brucei* cells reported by Coppens et al. by 3-HMG-CoA reductase enzymatic inhibitors [58]. This indicates an essentiality of the mevalonate producing biosynthetic pathway or an essentiality of mevalonate itself due to its role not only in membrane biogenesis through the production of sterols, mainly ergosterol and cholesterol in procyclics and bloodstream forms respectively, but also in the generation of mevalonate successors involved in other biological processes like the transport of electrons, RNA translocation or the attachment of polypeptides to cell walls [58,63].

The incomplete knockdown of protein expression in the Tb13600 and the errors during the WB of Tb840 growth curve samples would require a repetition of these RNAi experiments. Additionally, RNAi ablation of Tb4540 in bloodstream forms would expand the data regarding the essentiality of this protein in this developmental stage, and lead to further investigations of this protein as a potential medicinal target for the treatment of HAT and AAT. Previous studies applying pharmaceutical agents reacting with compounds present in the sterol biosynthetic pathway against trypanosomatids led to detectable growth defects and animal trials showed varying degrees of efficacy for some of these drugs. However, as of 2009, these

studies have yet to be repeated for *T. brucei* specifically or had no reported application in human trials [63].

6 Conclusion

One main aim of this thesis was to further investigate the mitochondrial TAC relation from the TrypTag database for Tb13600, Tb14570, Tb840 and Tb4540 through endogenous tagging with the 3xV5 epitope at the C-terminus with subsequent localization by IFA and WB of subcellular fractionated samples. Additionally, given that for the prioritized proteins this was not addressed before, genetic knockdown studies of the genes of interest *via* RNAi were conducted to assess the relevance of these proteins on the growth of this parasite in its procyclic form.

Both the IFA and WBs analyses located the examined proteins within the mitochondrion. However, their TAC relations could not be verified. Our results suggest that these previous TAC localizations are artifactual instead. Although these results do not validate the TAC localization of the studied proteins, and therefore not expand the known TAC components, they provide an example about the cautions that must be taken when assessing subcellular localization based on the evaluation of a unique epitope tag instead.

As for the essentiality of the studied proteins, the tetracycline induced RNAi led to an observable decrease in of protein expression of Tb13600. This instigated only a minor change in cell division, possibly caused by the incomplete knockdown of the protein. Knockdown of Tb14570 resulted in no apparent growth defect after total suppression of protein expression, indicating a possible functional redundancy. RNAi of Tb840 brought about an apparent growth decrease. The accompanying WB was inconclusive due to errors during the execution of the experiment, preventing the interpretation of this investigation.
Downregulation of the protein Tb4540 led to a suspension of cell division after 6 days of tetracycline induction. Subsequent WB indicated the complete knockdown of protein expression. These results suggest an essentiality of this protein for procyclic *T. brucei* and are in accordance with the results a previous experimental drug induced suppression, pointing the mevalonate and sterol synthesis pathway as appealing drug targets for the interventions against trypanosomatid-driven health-threatening diseases [58,63].

7 References

1. Achcar F, Kerkhoven EJ, Barrett MP. *Trypanosoma brucei*: Meet the system. Current Opinion in Microbiology. 2014;20: 162–169.
2. Matthews KR. The developmental cell biology of *Trypanosoma brucei.* Journal of Cell Science. 2005;118: 283–290.
3. Simarro PP, Jannin J, Cattand P. Eliminating human African trypanosomiasis: Where do we stand and what comes next? PLoS Medicine. 2008;5: 174–180.
4. Rijo-Ferreira F, Takahashi JS. Sleeping Sickness: A Tale of Two Clocks. Frontiers in Cellular and Infection Microbiology. 2020;10: 1-10.
5. Zhang X, An T, Pham KTM, Lun Z-R, Li Z. Functional Analyses of Cytokinesis Regulators in Bloodstream Stage *Trypanosoma brucei* Parasites Identify Functions and Regulations Specific to the Life Cycle Stage. mSphere. 2019;4: 1-14.
6. Wheeler RJ, Gull K, Sunter JD. Coordination of the Cell Cycle in Trypanosomes. Annual Review of Microbiology. 2019;73: 133-154.
7. de Souza W. Special organelles of some pathogenic protozoa. Parasitology Research. 2002;88: 1013–1025.
8. Zíková A. Mitochondrial adaptations throughout the *Trypanosoma brucei* life cycle . Journal of Eukaryotic Microbiology. 2022;e12911: 1-19.
9. Bauer S, Morris MT. Glycosome biogenesis in trypanosomes and the de novo dilemma. PLoS Neglected Tropical Diseases. 2017;4: 1-13.
10. Michels PAM, Bringaud F, Herman M, Hannaert V. Metabolic functions of glycosomes in trypanosomatids. Biochimica et Biophysica Acta. 2006;1763: 1463–1477.
11. Procházková M, Panicucci B, Zíková A. Cultured bloodstream *Trypanosoma brucei* adapt to life without mitochondrial translation release factor 1. Scientific Reports. 2018;8: 1-15.
12. Matthews KR. 25 years of African trypanosome research: From description to molecular dissection and new drug discovery. Molecular and Biochemical Parasitology. 2015;200: 30–40.
13. Jakob M, Hoffmann A, Amodeo S, Peitsch C, Zuber B, Ochsenreiter T. Mitochondrial growth during the cell cycle of *Trypanosoma brucei* bloodstream forms. Scientific Reports. 2016;6: 1-13.

14. Beck K, Acestor N, Schulfer A, Anupama A, Carnes J, Panigrahi AK, et al. *Trypanosoma brucei* Tb927.2.6100 is an essential protein associated with kinetoplast DNA. Eukaryotic Cell. 2013;12: 970–978.
15. Bílý T, Sheikh S, Mallet A, Bastin P, Pérez-Morga D, Lukeš J, et al. Ultrastructural Changes of the Mitochondrion During the Life Cycle of *Trypanosoma brucei*. Journal of Eukaryotic Microbiology. 2021;68: 1-11.
16. Hoffmann A, Käser S, Jakob M, Amodeo S, Peitsch C, Týc J, et al. Molecular model of the mitochondrial genome segregation machinery in *Trypanosoma brucei*. PNAS. 2018;115: 1809–1818.
17. Baudouin HCM, Pfeiffer L, Ochsenreiter T. A comparison of three approaches for the discovery of novel tripartite attachment complex proteins in *Trypanosoma brucei*. PLoS Neglected Tropical Diseases. 2020;14: 1–21.
18. Schneider A, Ochsenreiter T. Failure is not an option - mitochondrial genome segregation in trypanosomes. Journal of Cell Science. 2018;131: 1-9.
19. Aslett M, Aurrecoechea C, Berriman M, Brestelli J, Brunk BP, Carrington M, et al. TriTrypDB: A functional genomic resource for the Trypanosomatidae. Nucleic Acids Research. 2009;38: 457-462.
20. Dean S, Sunter JD, Wheeler RJ. TrypTag.org: A Trypanosome Genome-wide Protein Localisation Resource. Trends in Parasitology. 2017;33: 80–82.
21. Panigrahi AK, Ogata Y, Zíková A, Anupama A, Dalley RA, Acestor N, et al. A comprehensive analysis of *Trypanosoma brucei* mitochondrial proteome. Proteomics. 2009;9: 434–450.
22. Stockmar I, Feddersen H, Cramer K, Gruber S, Jung K, Bramkamp M, et al. Optimization of sample preparation and green color imaging using the mNeonGreen fluorescent protein in bacterial cells for photoactivated localization microscopy. Scientific Reports. 2018;8: 1-11.
23. Poon SK, Peacock L, Gibson W, Gull K, Kelly S. A modular and optimized single marker system for generating *Trypanosoma brucei* cell lines expressing T7 RNA polymerase and the tetracycline repressor. Open Biology. 2012;2: 1-10.
24. Gomez-Martinez M, Schmitz D, Hergovich A. Generation of stable human cell lines with tetracycline-inducible (Tet-on) shRNA or cDNA expression. Journal of Visualized Experiments. 2013;73: 1-7.

25. Dean S, Sunter J, Wheeler RJ, Hodkinson I, Gluenz E, Gull K. A toolkit enabling efficient, scalable and reproducible gene tagging in trypanosomatids. Open Biology. 2015;5: 1-12.
26. Falschlehner C, Steinbrink S, Erdmann G, Boutros M. High-throughput RNAi screening to dissect cellular pathways: A how-to guide. Biotechnology Journal. 2010;5: 368–376.
27. McAllaster MR, Sinclair-Davis AN, Hilton NA, de Graffenried CL. A unified approach towards *Trypanosoma brucei* functional genomics using Gibson assembly. Molecular and Biochemical Parasitology. 2016;210: 13–21.
28. Gibson DG, Young L, Chuang RY, Venter JC, Hutchison CA, Smith HO. Enzymatic assembly of DNA molecules up to several hundred kilobases. Nature Methods. 2009;6: 343–345.
29. Atayde VD, Ullu E, Kolev NG. A single-cloning-step procedure for the generation of RNAi plasmids producing long stem-loop RNA. Molecular and Biochemical Parasitology. 2012;184: 55–58.
30. Handbook MinElute PCR Purification Kit. Qiagen. 2020.
31. Li S, Meadow Anderson L, Yang JM, Lin L, Yang H. DNA transformation via local heat shock. Applied Physics Letters. 2007;91: 1-3.
32. Rahimzadeh M, Sadeghizadeh M, Najafi F, Arab SS, Mobasheri H. MBRC Impact of heat shock step on bacterial transformation efficiency. Molecular Biology Research Communications. 2016;5: 257–261.
33. Bergkessel M, Guthrie C. Colony PCR. Methods in Enzymology. 2013;529: 299–309.
34. Handbook for Hybrid-Q^{TM} Plasmid Rapidprep Total DNA Purificiatin Kit. GeneAll Biotechnology. 2016.
35. Sayed N, Allawadhi P, Khurana A, Singh V, Navik U, Pasumarthi SK, et al. Gene therapy: Comprehensive overview and therapeutic applications. Life Sciences. 2022;294: 1-21.
36. Geng T, Zhan Y, Wang J, Lu C. Transfection of cells using flow-through electroporation based on constant voltage. Nature Protocols. 2011;6: 1192–1208.
37. Burkard G, Fragoso CM, Roditi I. Highly efficient stable transformation of bloodstream forms of *Trypanosoma brucei*. Molecular and Biochemical Parasitology. 2007;153: 220–223.
38. Novotná L. Functional analysis of subunit MRB3010 of the mitochondrial binding complex 1 in *Trypanosoma brucei*. Master Thesis. University of South Bohemia. 2010.

39. Lee PY, Costumbrado J, Hsu CY, Kim YH. Agarose gel electrophoresis for the separation of DNA fragments. Journal of Visualized Experiments. 2012;62: 1-5.
40. Dixit B, Batiuk E, Vanhoozer S, Anti NA, O'Connor MS, Boominathan A. Rapid enrichment of mitochondria from mammalian cell cultures using digitonin. MethodsX. 2021;8: 1-7.
41. Baghirova S, Hughes BG, Hendzel MJ, Schulz R. Sequential fractionation and isolation of subcellular proteins from tissue or cultured cells. MethodsX. 2015;2: 440–445.
42. Roy S, Kumar V. A Practical Approach on SDS PAGE for Separation of Protein. International Journal of Science and Research. 2014;3: 955-960.
43. Gwozdz T, Dorey K. Western Blot. In: Basic Science Methods for Clinical Researchers. 2017; 99–117.
44. Mahmood T, Yang PC. Western blot: Technique, theory, and trouble shooting. North American Journal of Medical Sciences. 2012;4: 429–434.
45. Martínez-Flores K, Tonatiuh Salazar-Anzures Á, Fernández-Torres J, Pineda C, Alberto Aguilar-González C, López-Reyes A, et al. Western blot: a tool in the biomedical field General interest. Investigación en Discapacidad. 2017;6: 128-137.
46. Yang L, Jin M, Du P, Chen G, Zhang C, Wang J, et al. Study on enhancement principle and stabilization for the luminol-H2O2-HRP chemiluminescence system. PLoS ONE. 2015;10: 1-14.
47. Im K, Mareninov S, Diaz MFP, Yong WH. An introduction to performing immunofluorescence staining. Methods in Molecular Biology. 2019;1897: 299–311.
48. Schneider CA, Rasband WS, Eliceiri KW. NIH Image to ImageJ: 25 years of image analysis. Nature Methods. 2012;9: 671–675.
49. Z Series Coulter Counter User manual. Beckman Coulter. 2004.
50. Ludewig MH, Boshoff A, Horn D, Blatch GL. *Trypanosoma brucei* J protein 2 is a stress inducible and essential Hsp40. International Journal of Biochemistry and Cell Biology. 2015;60: 93–98.
51. Kampinga HH, Andreasson C, Barducci A, Cheetham ME, Cyr D, Emanuelsson C, et al. Function, evolution, and structure of J-domain proteins. Cell Stress and Chaperones. 2019;24: 7–15.
52. Young NM, Foote SJ, Wakarchuk WW. Review of phosphocholine substituents on bacterial pathogen glycans: Synthesis, structures and interactions with host proteins. Molecular Immunology. 2013;56: 563–573.

53. Eberhardt A, Wu LJ, Errington J, Vollmer W, Veening JW. Cellular localization of choline-utilization proteins in *Streptococcus pneumoniae* using novel fluorescent reporter systems. Molecular Microbiology. 2009;74: 395–408.

54. Kuchta K, Knizewski L, Wyrwicz LS, Rychlewski L, Ginalski K. Comprehensive classification of nucleotidyltransferase fold proteins: Identification of novel families and their representatives in human. Nucleic Acids Research. 2009;37: 7701–7714.

55. Rinku D, Masayori I. GHKL, an emergent ATPase/kinase superfamily. Trends in Biochemical Sciences. 2000;25: 24-28.

56. Heises N, Opperdoes FR. Localisation of a 3-Hydroxy-3-methylglutaryl-Coenzyme A Reductase in the Mitochondrial Matrix of *Trypanosoma brucei* Procyclics. Zeitschrift für Naturforschung. 2000;55: 473-477.

57. Friesen JA, Rodwell VW. The 3-hydroxy-3-methylglutaryl coenzyme-A (HMG-CoA) reductases Gene organization and evolutionary history. Genome Biology. 2004;5: 1-7.

58. Coppens I, Bastin P, Levade T, Courtoy PJ. Activity, pharmacological inhibition and biological regulation of 3-hydroxy-3-methylglutaryl coenzyme A reductase in *Trypanosoma brucei*. Molecular and Biochemical Parasitology. 1995;69: 29-40.

59. Panicucci B, Gahura O, Zíková A. *Trypanosoma brucei* TbIF1 inhibits the essential F1-ATPase in the infectious form of the parasite. PLoS Neglected Tropical Diseases. 2017;11: 1-21.

60. Gasteiger E, Hoogland C, Gattiker A, Duvaud S, Wilkins MR, Appel RD, et al. Protein Analysis Tools on the ExPASy Server. The Proteomics Protocols Handbook. 2005; 571-607.

61. Peña-Diaz J, Montalvetti A, Flores CL, Constán A, Hurtado-Guerrero R, de Souza W, et al. Mitochondrial Localization of the Mevalonate Pathway Enzyme 3-Hydroxy-3-methyl-glutaryl-CoA Reductase in the Trypanosomatidae. Molecular Biology of the Cell. 2004;15: 1356–1363.

62. Alsford S, Turner DJ, Obado SO, Sanchez-Flores A, Glover L, Berriman M, et al. High-throughput phenotyping using parallel sequencing of RNA interference targets in the African trypanosome. Genome Research. 2011;21: 915–924.

63. de Souza W, Rodrigues JCF. Sterol Biosynthesis Pathway as Target for Anti-trypanosomatid Drugs. Interdisciplinary Perspectives on Infectious Diseases. 2009;2009: 1–19.